Methyl Formate and Its Mono and Difluoro Derivatives: Conformational Manifolds, Basicity, and Interaction with HF Theoretical Investigation

ARTICLE *in* THE JOURNAL OF PHYSICAL CHEMISTRY A · AUGUST 2011

Impact Factor: 2.69 · DOI: 10.1021/jp202981m · Source: PubMed

2 AUTHORS:

Thérèse Zeegers-Huyskens
University of Leuven
208 PUBLICATIONS **2,974** CITATIONS

SEE PROFILE

Eugene S Kryachko
University of Liège
139 PUBLICATIONS **2,026** CITATIONS

SEE PROFILE

THE JOURNAL OF PHYSICAL CHEMISTRY A

ARTICLE

pubs.acs.org/JPCA

Methyl Formate and Its Mono and Difluoro Derivatives: Conformational Manifolds, Basicity, and Interaction with HF Theoretical Investigation

Therèse Zeegers-Huyskens*,† and Eugene S. Kryachko*,‡

†Department of Chemistry, University of Leuven, 3001 Heverlee, Belgium

‡Bogolyubov Institute for Theoretical Physics, Kiev, 03680 Ukraine

Supporting Information

ABSTRACT: The conformational manifolds, scenarios of protonation, and hydrogen bond propensity of methyl formate and its mono and difluoro derivatives, which possess two oxygen atoms with different basicities, are studied at the B3LYP/6-311++G(3df,3pd) computational level. The optimized geometries of the title molecules, their energetics, and relevant harmonic vibrational frequencies, mainly of the ν(CH) mode of the H−C═O group, are of a primary focus. The Natural Bond Orbital analysis is invoked to obtain the second-order intra- or intermolecular hyperconjugation energies, occupations of antibonding orbitals, and hybridization of the carbon atoms. It is demonstrated that the *Z* conformers (and their rotamers) of the three title molecules are characterized by a higher stability compared to the *E* ones. The stabilities depend on the intramolecular hyperconjugative interaction and on the attraction or repulsion nonbonded interaction. The proton affinity of the carbonyl oxygen exceeds, by 15−20 kcal·mol^{-1}, that of the methoxy oxygen. Fluorine substitution causes a moderate lowering of the proton affinity of the oxygens. Protonation on the oxygen atoms yields a contraction of the C−H bond and large concomitant blue shift of the ν(CH) vibration. These changes are mainly determined by a lowering of the occupation of the corresponding σ^*(CH) orbitals. The esters under consideration are probed on the interaction with the HF molecule. The complexes that are formed under this interaction on the oxygen of the H−C═O group are stronger than those formed on the oxygen belonging to the methoxy one. It is deduced that the hydrogen bond energies show a linear dependence on the proton affinities of the corresponding oxygen atoms. Hydrogen-bonded complexes of moderate strength are also formed, while HF interacts with the fluorine atoms of the fluorinated esters.

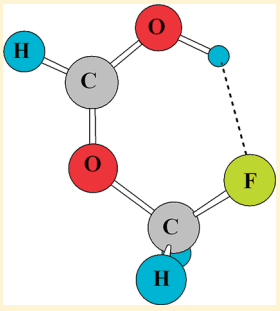

1. INTRODUCTION

The hydrogen bond is definitely one of the key domains of molecular interactions that plays a vital role in the diverse variety of physical, chemical, and biological processes.[1] By definition,[1] the hydrogen bonding interaction involves three bodies: two proton acceptors A and B and a hydrogen atom H that is shared between them, either in the configuration A−H···B or in A···H−B, whose preference is largely governed by a mutual interplay of electronegativities of A and B. The oxygen atom is a typical conventional proton acceptor − say B in the above configuration A−H···B − that is often entangled via R−O−R′ with side groups, as, for example, in C═O and C−O−C, and often subjected to substitution. There was much research focused on the hydrogen bonds either formed on the former, carbonyl's, or the latter, ether's, oxygen atom.[1,2] The strength of these bonds appeared to be quite sensitive to the nature of R-substituents directly implanted on the O atom. One of the powerful approaches to investigate the hydrogen bond is definitely the Bader's Quantum Theory of Atoms in Molecules[3,4] (QTAIM, see also, ref 5) that uses the concepts of the bond paths and bond critical points (BCPs) of the H···B bonds. The key QTAIM's conjecture is the existence of the relationship between the one-electron density $\rho_{H\cdots B}(\mathbf{r}_{BCP})$ and its Laplacian $\nabla_{\mathbf{r}}^2\rho_{H\cdots B}(\mathbf{r}_{BCP})$, on the one hand, and the hydrogen bonding energy, on the other. Hence, together with $\rho_{A-H}(\mathbf{r}_{BCP}')$ and its Laplacian $\nabla_{\mathbf{r}}^2\rho_{A-H}(\mathbf{r}_{BCP}')$, these latter quantities measure the hydrogen bond strength. The other suggestion is that the Laplacian $\nabla_{\mathbf{r}}^2\rho$ may cast as the indicator of the preferable site of protonation.[2a]

Much less studies have been however conducted on those molecules that simultaneously have two nonequivalent O atoms characterized by different basicity. Ester derivatives belong, for example, to this class. Aliphatic esters were the concern of the early works.[6−8] According to IR spectroscopic[6] and computational[7] studies, both oxygen atoms of methyl acetate are involved in the interaction with HCl. It was also computationally demonstrated[8,9] that, in methyl formate and methyl acetate and formic acid, both oxygens take part in the interaction with water and HF, respectively.

The hydrogen bond affinity of methyl formate, O═CHOCH$_3$, and its mono and difluoro derivatives, O═CHOCH$_2$F and O═CHOCHF$_2$, is the key theme of the present investigation. A number of factors rule this affinity, among which a conformational manifold is definitely not the last. While two conformations are admitted by methyl formate,[10−15] the conformational manifolds of mono and difluoro formates still remain unknown.

Special Issue: Richard F. W. Bader Festschrift

Received: March 31, 2011
Revised: August 1, 2011
Published: August 19, 2011

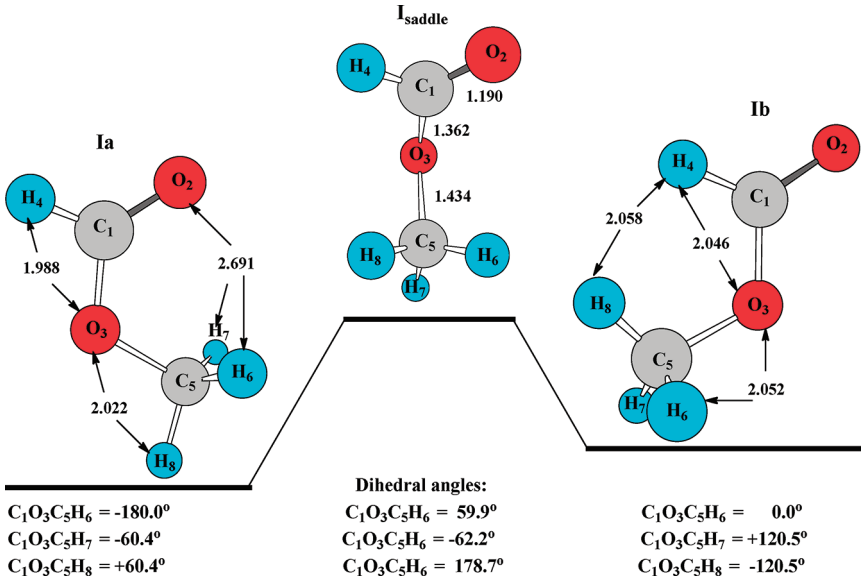

Figure 1. Conformational manifold of methyl formate with a pair of the oxygen atoms: O_2 belonging to the carbonyl group $H_4-C_1=O_2$ and O_3 of the ether group $C_1-O_3-C_5H_{6-8}$. The transition frequency of $\mathbf{I_{saddle}}$ is equal to 246*i* and 256*i* cm^{-1} for $MP2_{fc}$ and B3LYP, respectively.

Notice, in this regard, that the conformations of halogenated esters, trifluoromethyl formate,[15] trifluoromethyl chloroformate, or chloroacetate[16] were studied, both experimentally and computationally.

The present paper endows the following layout. Section 2 aims to study, in a consistent manner, the conformational manifolds of methyl- and fluoroformates from different angles of view, including the hyperconjugative and dipole−dipole interactions. Because the basicity of the constituting atoms is directly linked to the hydrogen-bond affinity, section 3 focuses on the protonation of the title molecules and the proton affinity, PA, of their two oxygens. Under protonation, the proton forms an $O-H^+$ bond, which electron delocalization is discussed in depth and compared with that of the neutral parent molecules. Section 4 examines the properties of the complexes resulted from the interaction with HF, partly establishing a correlation between their enthalpies of formation and the PAs of the oxygens. A particular attention is drawn therein to the blue shift of the ν(CH) vibration of the H−C=O group in the protonated and hydrogen-bonded complexes. Recall shortly that the origin of blue shifts of the C−H bond involved in the hydrogen bonding interaction fundamentally resembles the red one and its shift sign results from a subtle balance of concurrent effects,[17] though, speaking generally, blue shifts may also occur in the C−H groups that do not directly participate in a hydrogen bond.[18]

2. COMPUTATIONAL METHODOLOGY

All calculations of the esters, their isomers, or rotamers, reported in the present work, were performed within the density functional B3LYP using the Gaussian suite of programs.[19] The basis set 6-311++G(3df,3pd) was invoked. The second-order perturbation Møller−Plesset frozen-core method ($MP2_{fc}$) was also used to "control", in a sense, the computational adequacy. All geometry optimizations were carried out with the TIGHT option. The harmonic vibrational frequencies of these complexes were calculated to properly characterize stationary points and to obtain the zero-point energy (ZPE). Thermodynamic quantities, such as enthalpies and entropies, were estimated from the partition functions calculated at room temperature (298.15 K) using the Boltzmann thermostatistics and the rigid-rotor-harmonic-oscillator approximation. The effect of the counterpoise correction[20] to the basis set superposition error, BSSE, was not taken into account because the previous and related computational studies demonstrate that the explicit inclusion of these corrections does not substantially change the discussed trends.

The proton affinity was calculated as the negative enthalpy of the protonation reaction under the standard conditions in the gas phase. The hydrogen bond energies of the HF complexes include the ZPE corrections. The natural bond orbital, NBO for short, analysis[21] was also conducted to shed light on a variety of interaction features. The intramolecular hyperconjugative interaction energies (HYPE) between different lone pairs of the O or F atoms and different antibonding orbitals were estimated within the second-order perturbation theory. Intermolecular charge transfer effects that occur under protonation were treated as well.

3. RESULTS AND DISCUSSION

3A. Methyl Formate. *3A.1. Structures and Energies.* The conformational manifold of methyl formate molecule CH_3O-COH, computationally investigated in the past,[10−12,15b] contains two conformers or rotamers, *Z*(**Ia**) and *E*(**Ib**), both displayed in Figure 1. Their selected distances and bond angles are listed in Table 1. The key factor that distinguishes *Z* and *E* from each other is the dihedral angle $\angle O_2C_1O_3C_5$ that for *Z* is equal to 0° and 180° for *E*. A rotation of the methyl group yields two different rotamers, staggered and eclipsed, with respect to the carbonyl group. In the former, $\angle C_1O_3C_5H_6 = -180°$, that is, the C_5H_6 bond is "*cis*" to the O_3's lone pairs (LPs), whereas in the latter, it is zero; the C_5H_6 bond is "*gauche*" to the O_3 LPs.

Z appears to be a more stable conformer than *E*.[22] Their experimental difference in energy,[13] comprised of 4.75 ± 0.19 kcal·mol^{-1}, is rather accurately accounted for by the invoked B3LYP and $MP2_{fc}$ levels yielding 4.55 and 5.49 kcal·mol^{-1} without (Table 2) and 4.09 and 4.87 kcal·mol^{-1} with the ZPE

Table 1. Selected Bond Lengths (Å) and Angles (deg.) of the Conformers of O=CHCOCH$_3$, O=CHOCH$_2$F, and O=CHOCHF$_2$ and Frequencies (cm^{-1}) of the Stretching Vibrations of the C$_1$−H$_4$ and C=O Bonds

	O=CHOCH$_3$		O=CHOCH$_2$F			O=CHOCHF$_2$		
	Ia	**Ib**	**IIa**	**IIb**	**IIc**	**IIIa**	**IIIb**	**IIIc**
Geometry								
C$_1$=O$_2$	1.199	1.192	1.192	1.198	1.186	1.191	1.185	1.184
C$_1$−O$_3$	1.336	1.343	1.357	1.341	1.362	1.362	1.375	1.368
C$_1$−H$_4$	1.0969	1.1040	1.0955	1.0957	1.1020	1.0945	1.0956	1.1004
O$_3$−C$_5$	1.440	1.430	1.409	1.423	1.396	1.395	1.390	1.380
C$_5$−H$_6$, C$_5$−F$_6$	1.0880	1.0878	1.371	1.358	1.375	1.341	1.346	1.345
C$_5$−H$_7$, C$_5$−F$_7$	1.0880	1.0878	1.0863	1.0889	1.0861	1.347	1.346	1.345
C$_5$−H$_8$, C$_5$−F$_8$	1.0847	1.0912	1.0871	1.0889	1.0920	1.0866	1.088	1.0917
∠O$_2$C$_1$H$_4$	124.9	124.0	125.5	125.4	124.9	126.0	126.2	125.1
∠O$_3$C$_1$H$_4$	109.2	113.1	108.5	109.3	112.9	108.2	107.1	113.1
∠O$_2$C$_1$O$_3$	125.9	122.9	125.9	125.4	122.9	125.8	126.6	121.8
∠C$_1$O$_3$C$_5$	116.0	118.5	117.2	115.9	117.0	117.6	120.5	118.6
Frequencies								
ν(C$_1$H$_4$)	3042	2951	3061	3058	2977	3075	3060	2994
ν(C=O)	1795	1832	1821	1794	1864	1824	1849	1872

Table 2. B3LYP and MP2$_{fc}$ Relative Energies ΔE (kcal·mol^{-1}) and Dipole Moments μ (D) of the Conformers of Methyl Formate and Its Mono and Difluoro Derivatives

	O=CHOCH$_3$		O=CHOCH$_2$F			O=CHOCHF$_2$		
	Ia	**Ib**	**IIa**	**IIb**	**IIc**	**IIIa**	**IIIb**	**IIIc**
ΔE								
B3LYP	0[a]	4.55[c]	0[e]	1.28	2.80	0[g]	2.80	3.71
MP2$_{fc}$	0[b]	5.49[d]	0[f]	1.51	3.38	0[h]		4.36
μ								
B3LYP	1.96	4.29	2.28	0.39	3.54	1.39	2.94	3.22
MP2$_{fc}$	2.01	4.75	2.68	0.72	4.04	1.87		3.70

[a] Calculated energy E_{B3LYP} = −229.156293 E_h. [b] $E_{MP2_{fc}}$ = −228.681302 E_h. [c] Eclipsed rotamer. [d] Staggered rotamer. [e] E_{B3LYP} = −328.431251 E_h. [f] $E_{MP2_{fc}}$ = −327. 813754 E_h. [g] E_{B3LYP} = −427.715731 E_h. [h] $E_{MP2_{fc}}$ = −426.956834 E_h.

correction, correspondingly. The enthalpy difference ΔH between *Z* and *E* amounts are 4.28 and 5.17 kcal·mol^{-1}, respectively. Both of these values appear rather close to the experimental[13a] ΔH = 4.75 ± 0.19 kcal·mol^{-1}. *E* is separated from *Z* by the transition-state structure **I$_{saddle}$**, which is identified in this work and shown in Figure 1. Its barrier height relative to *Z* amounts to 14.0 kcal·mol^{-1} for the MP2$_{fc}$ and 13.4 kcal·mol^{-1} for the B3LYP. Both values fall within the experimental range of 10−15 kcal·mol^{-1}.[13a,15b] Altogether, this definitely gives credit to the chosen computational methodology. Within the MP2$_{fc}$ picture, the eclipsed rotamer of *E* is a saddle structure with a single imaginary frequency of 71*i* cm^{-1}, placed 0.2 kcal·mol^{-1} above the staggered *E*.

Their minimum-energy structures of the title fluoro-substituted methyl formates, which have not been studied so far to our knowledge, are computationally identified in the present work for the first time and are shown in Figures 2 and 3 and Figure A of Appendix. By direct analogy with methyl formate, the *Z* conformers of the mono and difluoro derivatives are more stable than their *E* counterparts (see Table 2). Actually, the potential energy surfaces (PESs) of these methyl formates are not exhausted by F-substitution(s) of the CH_3 group; it is demonstrated in Appendix A, they are not even the global energy minima. Interestingly, the **IIa**, **IIc**, **IIIa**, and **IIIc** conformers are not eclipsed, nor staggered, because the dihedral angles ∠C$_1$O$_3$C$_5$H$_6$(F$_6$) fall between 0° and 180°. These conformers are referred to hereafter as "distorted". The distorted rotamers **IIa** and **IIIa** are slightly more stable, by ∼1.3 and 2.8 kcal·mol^{-1}, respectively, than the staggered **IIb** and **IIIb** structures. The eclipsed structure **IIIc** with ∠C$_1$O$_3$C$_5$H$_8$ = 0°, which by the above definition has to be referred to as *E*, is actually the transition state with an imaginary frequency of 29*i* cm^{-1} that lies 0.7 kcal·mol^{-1} above the corresponding distorted structure. Therefore, the metastable *E*-conformer does not exist for difluoromethyl formate.

Regarding geometry, the *Z* conformers bear longer C=O and shorter C$_1$−O$_3$ bonds compared to the *E*'s, though **IIIb** is likely an exception. The C$_1$−H$_4$ and C$_5$−H$_8$ bonds are longer in *E*. ∠H$_4$C$_1$O$_2$ is practically insensitive to the conformation. In contrast, ∠H$_4$C$_1$O$_3$ increases by 4°−5° and ∠O$_2$C$_1$O$_3$ decreases by 3°−4° by passing from *Z* to *E*. All studied systems reveal a strong deviation from the tetrahedrality of the methoxy group, implying thus a broad variation of ∠O$_3$C$_5$H and ∠C$_5$O$_3$F within 105°−113°.

The harmonic frequencies of the ν(C$_1$H$_4$) and ν(C=O) stretching modes are given in Table 1. The experimental[23] frequencies are 2943 and 1754 cm^{-1}, which corresponds to a scale factor of ≈0.97, slightly better than the scale factor of 0.95 obtained from MP2/6-311G(d,p) calculations.[24] Both of these modes correlate with the corresponding distances.[25] The in-plane deformation mode of the C$_1$H$_4$ group is placed between 1380 and 1440 cm^{-1} and the out-of-plane between 1020 and 1040 cm^{-1}. Both modes are probably coupled. It is also valid for the ν(C$_1$O$_3$C$_5$) mode that falls within the 1200−1230 cm^{-1} interval.

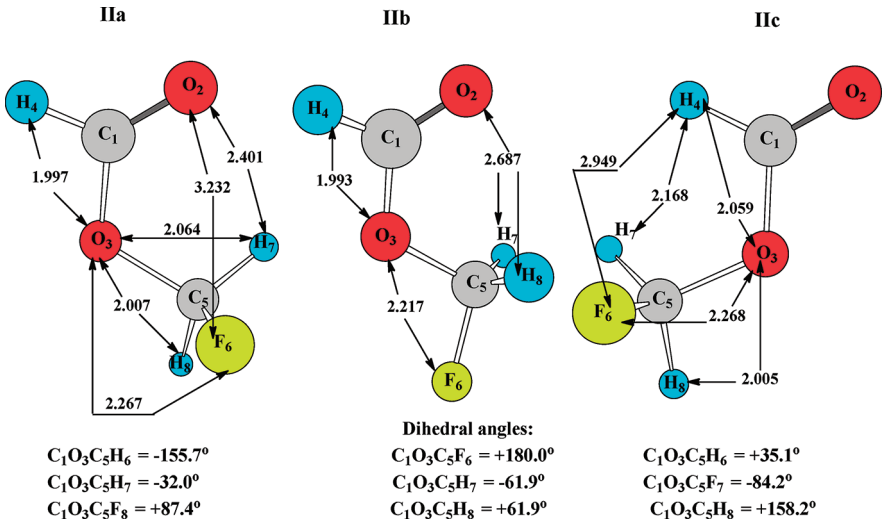

Figure 2. Portion of the B3LYP/6-31++G(3df,3dp)-conformational manifold of monofluoro-methyl formate **II**.

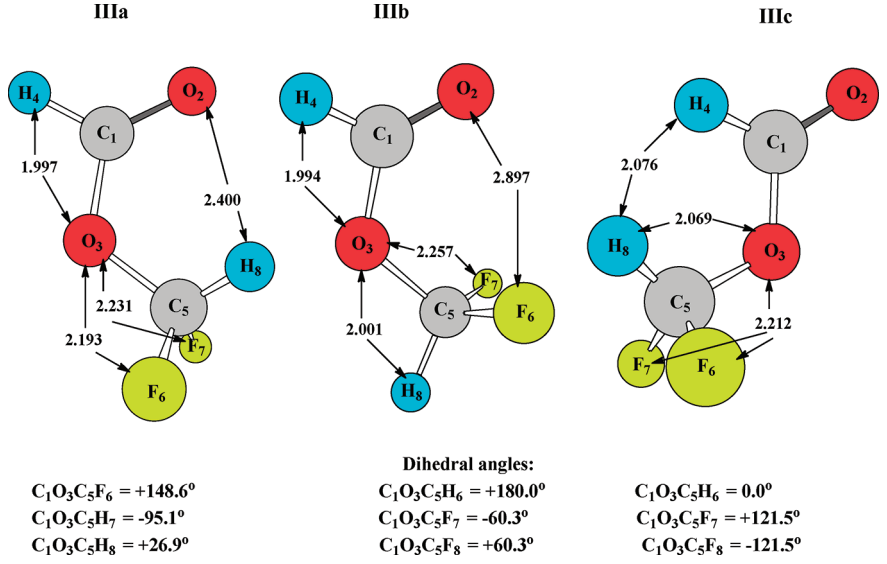

Figure 3. B3LYP/6-31++G(3df,3dp) optimized structures of the conformers of **III**.

3A.2. NBO Features. The NBO features, such as the NBO charges, occupation of relevant antibonding orbitals, hybridization of atoms, and hyperconjugation energies of methyl formates are gathered in Table 3. According to the classical theory of substitution, both O−CH_3 and F substituents are electron-giving by resonance effects and electron-attracting by inductive effects,[26] and both effects are reflected in the NBO characteristics. A lower hyperconjugation of *E* in comparison with *Z* is therefore predicted. A certain delocalization from the bonding orbitals to the antibonding, $\sigma(C_1H_4) \rightarrow \sigma^*(O_3C_5)$ and $\sigma(C_5H_8) \rightarrow \sigma^*(C_1O_3)$, ranges within 2−5 kcal·mol^{-1}. The two LPs of the O_3 atom, $sp^{1.5}$-hybridized [LP(1)] and p-hybridized [LP(2)], are delocalized over the CH_3 (CH_2F, CHF_2) groups and over the C═O bond of the esters, thus, implying that both effects have to be taken into account.

Below, we compare the esters and ethers and the bonding trends in the C_1-H_4, $C_1{=}O_2$ and C_1-O_3 bonds. Let us begin with the properties and bonding trends in the OCH_3, OCH_2F, and $OCHF_2$ groups of the ether[27,28] and ester derivatives. In dimethyl ether, the $C-H_{cis}$ bond is shorter than the other two CH_g bonds. According to the classical theory of the anomeric effect,[29] this difference is accounted by $n_O \rightarrow \sigma^*(CH_g)$ delocalization. In dimethyl ether, the LP(O) $\rightarrow \sigma^*$(CH) hyperconjugative interaction is stronger that in **Ia**, namely, 8.5 versus 4.4 kcal·mol^{-1} (Table 3). In CH_3OCH_2F, the LP(O) $\rightarrow \sigma^*$(CF) delocalization energy considerably exceeds that of **IIa** and **IIb**: 19.4 versus 13.8 and 5.6 kcal·mol^{-1}, respectively. In contrast to CH_3OCHF_2, the C−F bond in the ester is not in *gauche* position, meaning a repulsion between the negatively charged atoms F and O_2. Both **IIa** and **IIb** are stabilized by a weak intramolecular $C_5-H_7\cdots O_2$ hydrogen bond, the existence of which is resulted from a short intramolecular distance and a small hyperconjugation LP(O_2) $\rightarrow \sigma^*(C_5H_7)$ energy of ∼0.5−1 kcal·mol^{-1}. We suggest that the higher stability of **IIa** over **IIb** originates from a shorter $H_7\cdots O_2$ distance: 2.401 versus 2.687 Å, reflecting a somewhat stronger intramolecular H-bond in **IIa**.

Interestingly, the eclipsed structure of dimethyl ether possesses three equal C−H bonds[27] that is in contrast with the **Ib**

Table 3. Selected NBO Features: NBO Charges (e), Occupations of Antibonding Orbitals (e), Hybridization (% s character), and Hyperconjugation Energies (kcal·mol^{-1}) ≥ 0.5 kcal·mol^{-1} (Otherwise "u" for Undefined)[a]

	O=CHOCH$_3$		O=CHOCH$_2$F			O=CHOCHF$_2$		
	Ia	**Ib**	**IIa**	**IIb**	**IIc**	**IIIa**	**IIIb**	**IIIc**
Charge								
C_1	0.682	0.685	0.690	0.679	0.686	0.688	0.685	0.683
O_2	−0.591	−0.559	−0.565	−0.585	−0.531	−0.559	−0.529	−0.517
H_4	0.111	0.083	0.119	0.120	0.095	0.125	0.121	0.098
O_3	−0.548	−0.548	−0.566	−0.556	−0.557	−0.569	−0.589	−0.557
C_5	−0.210	−0.196	0.388	0.406	0.392	0.881	0.890	0.883
H_6	0.184	0.183	0.151		0.156		0.130	
F_6				−0.367		−0.351		−0.353
H_7	0.186	0.183		0.151				
F_7			−0.378		−0.382	−0.357	−0.354	−0.353
H_8	0.186	0.168	0.161	0.151	0.136	0.141		0.115
F_8							−0.354	
Hybridization								
(1)$C_1(O_2)$	36.3	36.4	35.4	36.2	36.3	32.3	36.4	36.8
(2)$C_1(O_2)$	0	0	0.8	0	0	4.0	0	0
$C_1(O_3)$	29.6	29.2	29.0	29.2	28.5	28.6	31.7	28.1
$C_1(H_4)$	34.7	34.9	35.4	35.2	35.4	35.7	35.8	35.6
$C_5(O_3)$	20.9	21.4	22.7	22.3	23.6	24.2	25.2	28.7
$C_5(H_6)$	25.9	26.2	27.6		27.8		29.4	
$C_5(H_7)$	26.7	26.2		28.4				
$C_5(H_8)$	26.7	26.3	28.7	28.4	27.9	30.2		29.6
$C_5(F_6)$				21.4		22.7	22.9	22.8
$C_5(F_7)$			21.5		21.3	22.8	22.9	22.9
Hyperconjugation Energy								
LP(2)O_2[b] → $\sigma^*(C_1O_3)$	32.7	34.1	35.2	33.5	36.6	36.3	39.2	38.1
→ $\sigma^*(C_1H_4)$	21.3	22.5	21.2	21.1	22.5	21.0	21.4	22.6
LP(1)O_3[c] → $\sigma^*(C_1O_2)$	6.7	2.8	6.5	6.4	2.6	6.1	6.3	2.6
→ $\sigma^*(C_5F_6)$				5.6		4.2		1.9
LP(2)O_3[b] → $\pi^*(C_1O_2)$	50.4	46.5	40.6	48.4	39.3	31.3	38.3	38.6
→ $\sigma^*(C_5H_6)$	2.4	4.3	0.8					
→ $\sigma^*(C_5H_7)$	4.4	4.3		4.7				
→ $\sigma^*(C_5H_8)$	4.4	u	1.5	4.7	2.0	u		u
→ $\sigma^*(C_5F_6)$				u		3.4	10.4	10.7
→ $\sigma^*(C_5F_7)$			13.8		15.7	13.5	10.4	10.7
LP(3)F_6[b] → $\sigma^*(O_3C_5)$			12.6	12.5	12.5	6.5	6.5	7.1
LP(3)F_7[b] → $\sigma^*(O_3C_5)$							6.3	7.1
$\pi^*(C_1O_2)$ → $\sigma^*(C_1O_2)$						8.6		
LP(1)O_2 → RY*C_1	14.4	16.7	14.9	17.0	15.1	15.1	15.1	16.8
Antibonding Orbital: Occupation								
$\sigma^*(C_1O_2)$	0.014	0.011	0.016	0.013	0.010	0.028	0.012	0.009
$\pi^*(C_1O_2)$	0.196	0.187	0.159	0.187	0.149	0.143	0.138	0.145
$\sigma^*(C_1O_3)$	0.096	0.100	0.108	0.096	0.109	0.108	0.120	0.114
$\sigma^*(C_1H_4)$	0.063	0.078	0.061	0.062	0.075	0.060	0.062	0.074
$\sigma^*(O_3C_5)$	0.020	0.015	0.053	0.052	0.046	0.077	0.080	0.073
$\sigma^*(C_5H_6)$	0.013	0.013	0.026		0.026		0.044	
$\sigma^*(C_5H_7)$	0.013	0.013		0.030	0.033			
$\sigma^*(C_5H_8)$	0.009	0.015	0.029	0.030		0.046		0.053
$\sigma^*(C_5F_6)$				0.026		0.067		0.080
$\sigma^*(C_5F_7)$			0.046		0.055	0.078	0.078	0.087
$\sigma^*(C_5F_8)$							0.078	

[a] The hyperconjugation energies of the *Z* rotamer of methyl formate were calculated at the HF/3-21G computational level:[9] the LP(2)O_3 → π^*(C=O) and LP(2)O_2 → $\sigma^*(C_1O_3)$ delocalization energies exceed the present ones by about 20 kcal·mol^{-1}. [b] Pure p orbital. [c] $sp^{1.5}$ orbital.

dx.doi.org/10.1021/jp202981m |*J. Phys. Chem. A* 2011, 115, 12586–12601

structure of methyl formate which C_5-H_8 bond is longer than the two others, despite a negligible delocalization from the $LP(O_3)$ to the $\sigma^*(C_5H_8)$ orbital and the same hybridization (26.2% s-character) of the C_5 atom bonded to the three H atoms. This behavior appears somewhat intriguing and is tentatively explained by the repulsion of positively charged H_4 and H_8 atoms separated by a short distance of 2.058 Å. Similar short $H_4\cdots H_8$ distances occur in **IIc** and **IIIc**.

In the fluorinated esters, we observe the following: the $\sigma^*(CH)$ occupation falls within 0.026−0.053 e, the occupation of the $\sigma^*(CF)$ orbital is larger, within 0.026−0.087 e, that is in agreement with larger $n_{O3} \rightarrow \sigma^*(CF)$ delocalization energies comparing with the $n_{O3} \rightarrow \sigma^*(CH)$ ones. This yields a larger σ^*-acceptor ability of the C−F bond than the C−H one that lies in agreement with the early computational data.[30] The π-donor ability of F is determined by the $LP(3)F_6(F_7) \rightarrow \sigma^*(O_3C_5)$ delocalization. Note, in this regard, that F atoms of fluorinated ketones are treated as poor π-donors,[10] in contrast to the fluorinated esters. The acceptor ability of the C−F bond, which is determined by the $LPO_3(2) \rightarrow \sigma^*(CF)$ delocalization, is somewhat larger than its π-donor ability. This observation is in accord with the classical inductive and resonance parameters of the F atom, $\sigma_I = 0.52$ and $\sigma_R = -0.25$[26] and in good agreement with fluoromethanol.[31] In this molecule, the $LP(2)O \rightarrow \sigma^*(CF)$ conjugation energy amounts to 23 kcal·mol^{-1}. This value is about twice the $LPF(3) \rightarrow \sigma^*(CO)$ value predicted for the **IIa** conformer of the monofluorinated ester (Table 3).

Let us move one step further and examine the factors which determine the C−H and C−F bond lengths. It is generally accepted that there are two key factors that act in opposite directions, namely, Factor 1, an increase of s-character of C at H(F) that contracts the C−H(F) bond; Factor 2, an increase in the occupation of the $\sigma^*(CH)$ orbital that elongates it. Their intercorrelations are given elsewhere.[32] The present study demonstrates that the C_1-H_4 bonds are longer in *E* rather in *Z*, which is in parallel with a slightly larger, by about 0.015 e, $\sigma^*(C_1H_4)$ occupation and larger, by 1 kcal·mol^{-1}, $LP(2)O_2 \rightarrow \sigma^*(C_1H_4)$ hyperconjugation energy. The hybridization of the $C_1(H_4)$ atom is approximately equal for both conformers, meaning that the C_1-H_4 bond length is mainly determined by the $\sigma^*(C_1H_4)$ occupation (for the correlation, see section 3B). In contrast, the different C_5-H bond lengths do not reveal a full correlation with the NBO characteristics. That is readily seen from the nearly equal C_5-H_7 and C_5-H_8 distances in **IIc** and **IIIc** and the hybridization of $C_5(H_7H_8)$, though **IIc** is characterized by a substantially smaller $\sigma^*(CH)$ occupation of 0.033 e in comparison to **IIIc** with 0.053 e. A similar trend also holds for the C−F distances. Indeed, the shortest C−F distance of 1.345 Å is found in **IIIc**, which is characterized by the $\sigma^*(CF)$ occupation of 0.087 e and the longest C−F bond of 1.375 Å has a $\sigma^*(CF)$ occupation of 0.055 e. The C(F) hybridization varies within a narrow interval, between 21.3 and 22.9% s-character. One explains such an absence of correlation between bond lengths, on the one side, and the NBO features, on the other, by the intramolecular interaction, either attractive or repulsive, between nonbonded atoms. In halogenated ethers where the latter interaction is weaker, a quantitative relationship between the C−F distances and the corresponding $\sigma^*(CF)$ occupation does exist.[33]

Compare the variation of the C−H bonds in the title esters and in the chlorinated ethers.[31] In the latter, the C−H bonds are contracted under a Cl-substitution and this contraction well correlates with an increase of s-character at the C(H) atom, where the positive charges on the H atoms do increase correspondingly. This observation is in agreement with the Bent's rule[34] according to which the atomic s-character tends to localize on those orbitals which are directed toward electropositive groups and the p-character toward electronegative groups. In the molecules under consideration, the hybridization of $C_5(H)$ varies within a broad range, between 26% (**Ia**) and 30.7% (**IIIa**) *s*-character. However, in contrast to the chlorinated ethers, the positive charge on H decreases from 0.185 to 0.115 e when the s-character of C at H increases. This apparent anomaly is likely accounted for by different polarity of the C_5-H bonds. Indeed, in the chlorinated ethers, there exists an accumulation of negative charge on C leading to C^--H^+ polarity. On the contrary, the positive charge on C is essentially larger than that on H (in **IIa**, the charges vary between 0.388 and 0.151 e and in **IIIa** between 0.880 and 0.141 e), which is definitely a consequence of the larger electronegativity of F over Cl. Therefore, the Bent's rule is probably applicable if both atoms of the C−H groups are positively charged. Then, the atomic p-character tends to concentrate toward the less positively charged H atoms. For the strongly polarized C^+-F^- bonds, a decrease of p-character of C parallels that of the negative charges on F, as naturally anticipated.

Table 4. Proton Affinities (kcal·mol^{-1}) of the O_2, O_3, and F Atoms of the *Z* and *E* Conformers of Methyl Formate and its Mono and Difluoro Derivatives

	Ia	Ib	IIa	IIb	IIc	IIIa	IIIb	IIIc
O_2[a]	188.0	192.0	180.5	177.8	183.7	174.3	177.5	178.6
O_2[b]	186.0	190.3	176.5	175.0	184.9	173.1	175.8	179.9
O_3	167.1	170.5	161.1	162.3	163.3	154.2	156.0	159.0
F			165.4	166.7	165.8	163.9	165.9	171.1

[a] H^+ is *cis* to the C_1-H_4 bond. [b] H^+ is *trans* to this bond.

What can we learn for the carbonyl group? The NBO charge on its C_1 is quite insensitive to substituents and remains nearly constant, within 0.690−0.679 e, in all studied systems. The charge on O, however, decreases from −0.591 to −0.517 e upon fluorination. An elongation of the $C_1{=}O_2$ bond mirrors an increase of the $C_1{=}O_2$ polarity.[35] In all presented systems, the $LP(2)O_3 \rightarrow \pi^*(C_1{=}O_2)$ is the largest hyperconjugative interaction that decreases from 50.4 to 31.3 kcal·mol^{-1} upon fluorination. The $LP(1)O_3 \rightarrow \sigma^*(C_1{=}O_2)$ HYPEs ∈ (2.6, 6.7) kcal·mol^{-1} is smaller in *E* than in *Z*. The $C_1{=}O_2$ bond lengths are correlated with the sum of the two delocalization energies. This is discussed in the next subsection.

IIIa looks quite different. The $LP(2)O_3 \rightarrow \pi^*(C{=}O)$ delocalization is smaller, whereas the $\sigma^*(C{=}O)$ occupation and polarity of the C=O bond are larger compared with other mono- or difluorinated molecules. One also observes a different hybridization pattern of C_1 at O_2, which is nearly sp^2-hybridized in the (1)C=O bond and gains some s-character in the (2)C=O bond. A remarkable $\pi^*(C{=}O) \rightarrow \sigma^*(C{=}O)$ delocalization of ∼8 kcal·mol^{-1}, absent in the rest of the systems, deserves to be mentioned as well. Such departing behavior originates from the intramolecular $C_5-H_8\cdots O_2$ hydrogen bond, the existence of which is discussed above. The $LP(2)O_2 \rightarrow \sigma^*(C_1O_3)$ hyperconjugative interactions, contrasting with the main delocalization that is dominant in determining the C_1-O_3 bond length, are stronger. Upon fluorination, it is strengthened from 32.7 to 39.2 kcal·mol^{-1}. The HYPEs of the $LP(1)O_2$ to the first Rydberg orbital on C_1 are large too, falling within 14−17 kcal·mol^{-1}.

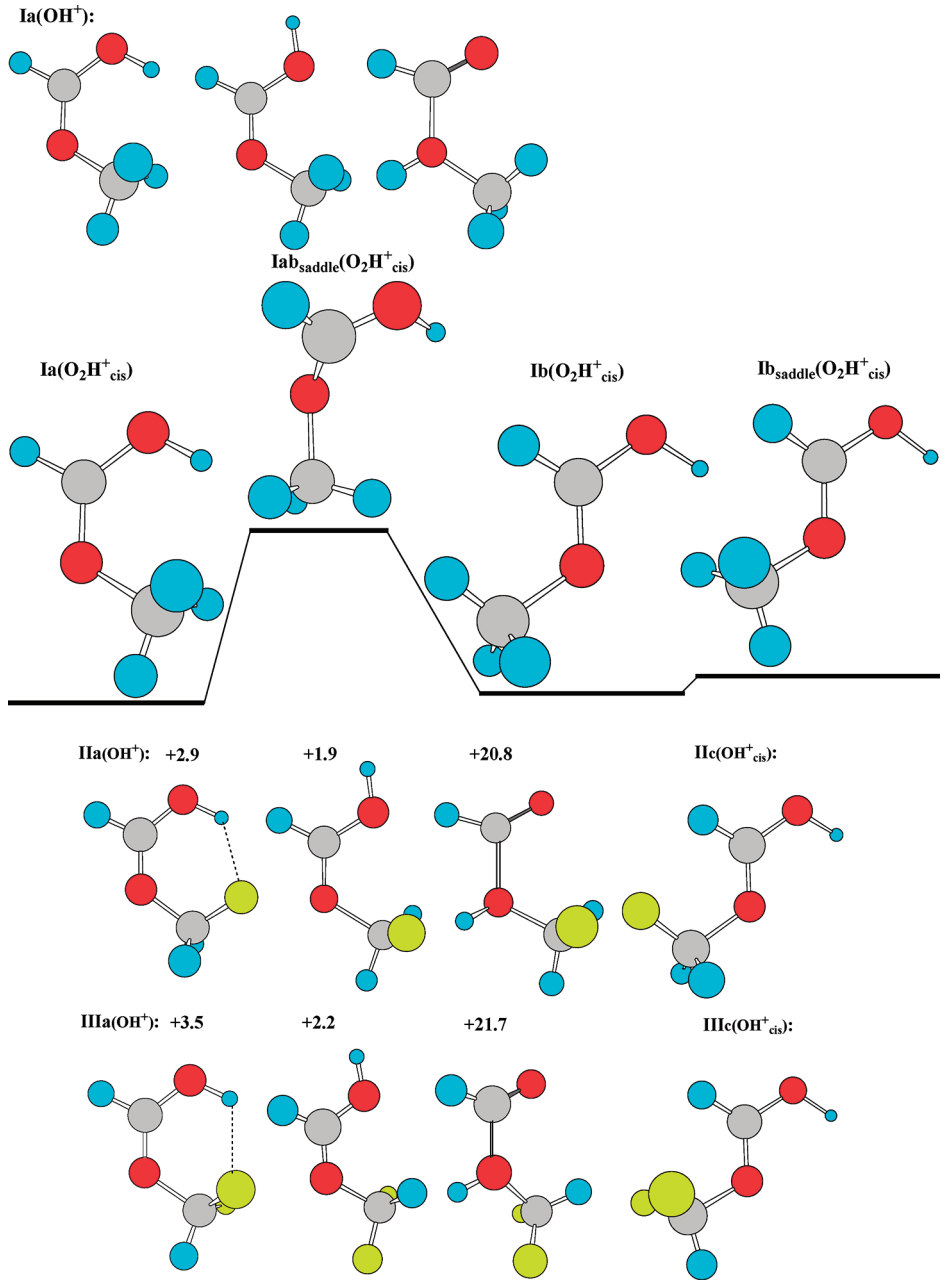

Figure 4. B3LYP/6-311++G(3d,f,3pd)-structures of **Ia**-, **IIa**-, and **IIIa**-protonated at the O_2 and O_3 atoms. Energy differences (in kcal·mol^{-1}) are taken relative to the global minimum energy conformer, which is **IIc**($O_2H^+_{cis}$) for **II** and **IIIc**($O_2H^+_{cis}$) for **III** (see eq 1). The upper panel describes the scenarios of the *cis*-protonation of **Ia** and **Ib** at O_2. The *cis*-protonation **Ib** at O_2 occurs indirectly via the transition structure **Ib**$_{saddle}$($O_2H^+_{cis}$) placed 0.5 kcal·mol^{-1} (B3LYP) above **Ib**($O_2H^+_{cis}$). The transition frequency of **Iab**$_{saddle}$($O_2H^+_{cis}$) is equal to 342*i* and 329*i* cm^{-1} for MP2$_{fc}$ and B3LYP, respectively. The B3LYP transition frequency of **Ib**$_{saddle}$($O_2H^+_{cis}$) is 122*i* cm^{-1}.

Their total effect on the relative stabilities of the esters is not so essential though.

The final question we pose, winding up this subsection, is what are the factors that rule the conformational manifolds of our systems? A large $n_{O3} \rightarrow \pi^*(C{=}O)$ hyperconjugative interaction in methyl formate explains a high stability of *Z* over *E*. A large delocalization of the LPO to the $\sigma^*(CF)$ orbital is also a key factor of a higher stability of the *gauche* conformer of fluoromethanol.[31] Fluorinated esters, however, do not reveal any relationship between the anomeric effect and the relative stabilities. The electrostatic theory[36] assumes that a conformation with a small dipole moment is favorable. According to Wiberg et al.,[8,10] a high stability of *Z* of methyl formate arises due to its dipole moment of 1.96 D, which is substantially smaller than that of 4.29 D of *E*. Hence, *Z* should be stabilized by the attractive interaction between the C═O and C−O dipoles. Such explanation is definitely valid for **IIa**−**IIc** and **IIIa**−**IIIc** pairs of conformers and fails for a slightly polar **IIb**, which the dipole moment is equal to 0.39 D only. These results show that the conformational stability is strongly determined by the intramolecular attraction or repulsion between the nonbonded atoms. The recent discussion of the anomeric effect in the OCO group of dimethoxy derivatives, which conformations

depend on the repulsion between the oxygen's LPs and the anomeric hydrogens,[37] is worth mentioning at the end.

3B. Protonation of Methyl Formate F-Derivatives. *3B.1. Proton Affinity.* The proton affinities of methyl formate and its fluoro-derivatives calculated in the present work are collected in Table 4 and partially obey the following inequalities:

$$\begin{aligned} 192.0\ \text{kcal}\cdot\text{mol}^{-1} &= \mathbf{Ib}(O_2H^+_{cis}) \overset{1.7}{>} \mathbf{Ib}(O_2H^+_{trans}) \\ &\overset{2.3}{>} \mathbf{Ia}(O_2H^+_{cis}) \overset{2.0}{>} \mathbf{Ia}(O_2H^+_{trans}) \overset{1.1}{>} \mathbf{IIc}(O_2H^+_{trans}) \\ &\overset{1.2}{>} \mathbf{IIc}(O_2H^+_{cis}) \overset{3.2}{>} \mathbf{IIa}(O_2H^+_{cis}) \overset{0.6}{>} \mathbf{IIIc}(O_2H^+_{trans}) \\ &\overset{1.3}{>} \mathbf{IIIc}(O_2H^+_{cis}) \overset{0.8}{>} \mathbf{IIb}(O_2H^+_{cis}) \overset{0.3}{>} \mathbf{IIIb}(O_2H^+_{cis}) \\ &\overset{1.0}{>} \mathbf{IIa}(O_2H^+_{trans}) \overset{0.7}{>} \mathbf{IIIb}(O_2H^+_{trans}) \overset{0.8}{>} \mathbf{IIb}(O_2H^+_{trans}) \\ &\overset{0.7}{>} \mathbf{IIIa}(O_2H^+_{cis}) \overset{1.2}{>} \mathbf{IIIa}(O_2H^+_{trans}) \overset{2.0}{>} \mathbf{IIIc}(FH^+) \\ &\overset{0.6}{>} \mathbf{Ib}(O_3H^+) = 170.5\ \text{kcal}\cdot\text{mol}^{-1} \end{aligned} \quad (1)$$

where the upper number indicates the difference in PAs between the left-hand-side structure and the right-hand-side one. The calculated value of the PA of methyl formate, 188.0 kcal·mol^{-1}, which is underlined in eq 1, is in a fair agreement with the PA^{expt} = 188.9 kcal·mol^{-1}.[37] Note that the approximate PA of single- and double-bonded O atoms can be obtained from the correlation between the PAs and the O(1s) core binding energies.[39] For methyl formate, this correlation yields PA = 187.7 kcal·mol^{-1} for C=O and 168.5 kcal·mol^{-1} for OCH_3, which are in good agreement, within 2 kcal·mol^{-1}, with Table 4 and eq 1, where the latter correlates with **Ib**(O_3H^+).

A number of observations are deduced from Table 4, eq 1, and Figure 4:

- The maximal PA of methyl formate, equal to 192.0 kcal·mol^{-1}, corresponds to **Ib**($O_2H^+_{cis}$), the protonated conformer *E*, which is, however, metastable,[22] compared to *Z*. Taking into account the difference in energy between *Z* and *E*, discussed in section 3A.1, this protonated conformer **Ib**($O_2H^+_{cis}$) and the other, **Ia**($O_2H^+_{cis}$), originated from the stable conformer *Z*, form a quasi energetic pair (see Figure 4), with a practically negligible offset of 0.2 kcal·mol^{-1} in a favor to the latter. On the PES of the protonated methyl formate, this looks like a nearly symmetric double well, separated by the barrier $\mathbf{I}_{saddle}(O_2H^+_{cis})$ of 18.8 kcal·mol^{-1} (ΔH = 17.8 kcal·mol^{-1}, MP2$_{fc}$) and 16.8 kcal·mol^{-1} (ΔH = 15.8 kcal·mol^{-1}, B3LYP) height. Therefore, the *cis*-protonation raises the barrier between *Z* and *E*. Generally speaking, in the studied systems, the PAs of the O_2 and O_3 atoms of *E* exceed, by ~3−8 kcal·mol^{-1}, those of the same atoms of *Z*. In a majority of protonation scenarios, the *cis*-protonation, that is, the protonation in the *cis* position with respect to the C_1−H_4 bond is slightly favored over the *trans* one. The structures of the O_2-protonated species are shown in Figure 4.
- Carbonyl protonation is favored over the acyl one by about 15−22 kcal·mol^{-1} (Figure 4).
- Acyl protonation of **IIIb** and **IIIc** induces a significant lengthening of the $C_1\cdots O_3$ bond to 1.811 and 1.828 Å, respectively, meaning its representation as [(HC=O)···($HOCHF_2^+$)]. We demonstrate this in Figure 5.
- As anticipated, the F-substitution lowers the PA of both O almost equally. The F atoms of the esters are expected to have basic properties, as inferred from their NBO charges varying between −0.353 and −0.383 e (see Table 3).

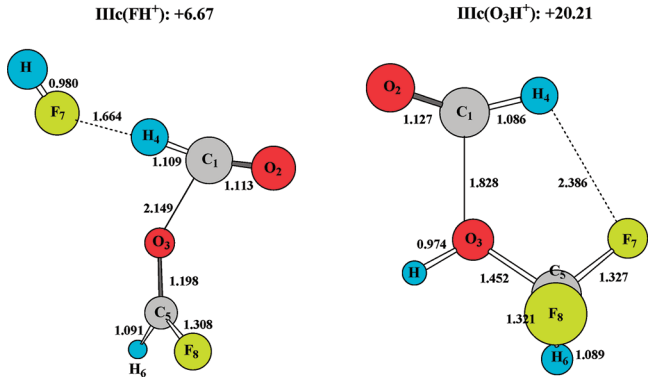

Figure 5. Protonated conformers **IIIc**(FH^+) and **IIIc**(O_3H^+). Energy differences (in kcal·mol^{-1}) are taken relative to the global minimum energy conformer **IIIc**($O_2H^+_{cis}$) (see eq 1).

According to the presented computational scenarios, the interaction of proton with one of the F atoms, either F_6 or F_7, causes a cleavage of the C−F bonds, elongated from 1.345−1.375 Å to 2.440−2.537 Å, and the formation of the metastable complexes [(O=CHOCH)$^+\cdots$HF] or [(O=CHOCF)$^+\cdots$HF], respectively. The latter are characterized by slightly elongated H−F bonds: 0.927−0.931 Å versus 0.922 Å in the isolated molecule. The F-protonated **IIIc**(FH^+) system, shown in Figure 5 and yielding, according to eq 1, the largest PA(F), which exceeds the largest PA(O_3), is actually a ternary complex [$(CHFO)^{+0.12}\cdots(C{=}OH)^{+0.84}\cdots(FH)^{+0.04}$], where the $O_3\cdots C_1$ bond is significantly elongated to 2.149 Å and F_7 is hydrogen-bonded to H_4. The dissociation of the C_5−F_7 bond that results from protonation at the F atom(s) has been recently found in a number of molecular systems.[40] It is worth mentioning in this regard that the PAs of the O-acyl are lower by 12−16 kcal·mol^{-1} compared to the PAs of the corresponding fluorinated ethers.[28] The PA of the carbonyl O atom of methyl formate is larger than that of H_2C=O, which amounts to 175 kcal·mol^{-1}, and of CH_3HC=O, equal to 183.7 kcal·mol^{-1}.[38]

3B.2. Structures and NBO Features of Protonated Conformers. In the O-protonated molecules, one of the LPs of O is tied up in the formation of the O−H^+ bond and, as a consequence, the hyperconjugation from this LP to the adjacent bonds vanishes. In the esters, protonation at one of the O atoms may perturb the hyperconjugation from the LPs of the second O atom to the adjacent bonds. Therefore, this protonation scenario is rather convenient to discuss the anomeric effect, especially in the esters. For this purpose, let us analyze the geometric (Tables 5 and S1 of the Supporting Information) and NBO (Table 6) characteristics of the most stable **Ia**, **IIa**, and **IIIa** conformers, protonated at the O_2 and O_3 atoms. We observe that the O−H^+ bond length varies between 0.974−0.978 Å and the corresponding ν(OH^+) vibrations between 3680−3622 cm^{-1}.[41] Note also that, in the C=OH^+ cations, the $H^+O_2C_1O_3$ skeleton is almost planar. In the O(CH_3)-protonated species, the proton is placed out of the $C_1O_3C_5$ plane by ~15°−20° (Figure 4).

Protonation of the C_1=O_2 bond naturally causes its elongation and contraction of the adjacent C_1−O_3. A reverse trend is observed if O_3 is protonated instead. In both situations, the O_3−C_5 bond is elongated. Protonation also causes dramatic changes of the bonding angles: (i) by analogy with the protonated

Table 5. Distances and Angles in the Ia, IIa, and IIIa Conformers Protonated at the O_2 and O_3 Atoms and Variations Induced by Protonation (in italics)[a]

	Ia(O_2H^+)[b]	Ia(O_3H^+)	IIa(O_2H^+)[b]	IIa(O_3H^+)	IIIa(O_2H^+)[b]	IIIa(O_3H^+)
$C_1{=}O_2$	1.276	1.151	1.268	1.145	1.265	1.142
	+0.077	*−0.048*	*+0.084*	*−0.047*	*+0.074*	*−0.048*
$C_1{-}O_3$	1.257	1.537	1.266	1.598	1.273	1.619
	−0.079	*+0.171*	*−0.091*	*+0.241*	*−0.089*	*+0.257*
$C_1{-}H_4$	1.0867	1.0904	1.0870	1.0894	1.0874	1.0890
	−0.0102	*−0.0065*	*−0.0085*	*−0.0061*	*−0.0071*	*−0.0055*
$O_3{-}C_5$	1.478	1.502	1.465	1.496	1.479	1.513
	+0.038	*+0.062*	*+0.056*	*+0.087*	*+0.084*	*+0.118*
$C_5{-}H_6$	1.0825	1.0837	1.0852	1.0871		
	−0.0022	*−0.0010*	*−0.0011*	*−0.0008*		
$C_5{-}H_8$	1.0877	1.0841	1.0872	1.0860	1.0861	1.0870
	−0.0003	*−0.0039*	*−0.0001*	*−0.0009*	*−0.0005*	*−0.0004*
$C_5{-}F_6$			1.354	1.329	1.313	1.308
			−0.017	*−0.042*	*−0.033*	*−0.031*
$C_5{-}F_7$					1.331	1.308
					−0.017	*−0.038*
$\angle C_1O_2C_5$	123.3	122.4	127.4	120.1	124.2	122.1
	+7.3	*+6.4*	*+10.2*	*+2.9*	*+6.6*	*+5.1*
$\angle O_2C_1O_3$	127.6	117.9	128.4	116.9	128.4	116.8
	+1.7	*−8.0*	*+2.5*	*−9.0*	*+2.6*	*−9.0*
$\angle O_2C_1H_4$	115.7	135.4	116.1	137.1	116.1	138.6
	−9.2	*+10.5*	*−9.4*	*+11.6*	*−9.9*	*+12.6*
$\angle O_3C_1H_4$	116.7	106.6	115.4	105.5	115.6	104.5
	+7.5	*−2.6*	*+7.0*	*-3.0*	*+7.4*	*−3.7*
OH^+	0.9740	0.9731	0.9786	0.9757	0.9775	0.9782
$\Delta\nu(C_1H_4)$	+152	+113	+128	+111	+113	+101
$\nu(C{=}O)$	[c]	1993	[c]	2024	[c]	2033
		198		*203*		*209*
$\nu(OH^+)$	3680	3684	3600	3652	3628	3622

[a] Frequencies of the $\nu(C_1H_4)$, $\nu(C{=}O)$, and $\nu(OH^+)$ vibrational modes (cm^{-1}). [b] H^+ *trans* to the $C_1{-}H_4$ bond. [c] See discussion in the text.

ethers,[6,28] there occurs an opening of $\angle C_1O_3C_5$; (ii) all angles in the neighborhood of C_1 undergo marked changes, among which the most spectacular is a decrease of $\angle O_2C_1H_4$ by ∼10° in the O_2H^+-protonated systems and an increase by >10° in the O_3H^+-protonated. Protonation induces a substantial contraction of the $C_1{-}H_4$ bonds, by 0.010−0.006 Å, and a large blue shift of 104−152 cm^{-1} of the $\nu(C_1H_4)$ vibration. Large perturbations of the $\nu(C{=}O)$ vibrations, which blue shifts reach about 200 cm^{-1}, are also worth noticing in the O_3-protonated systems. In the O_2H^+ cations, the vibrations are split into $\nu^{as}(O_2C_1O_3)$ and $\nu^{s}(O_2C_1O_3)$ components centered around 1650 and 1400 cm^{-1}. These vibrations are coupled to other modes, such as the in-plane deformation $\delta(C_1H_4)$. The $C_5{-}H$ and $C_5{-}F$ bonds undergo contraction, too.

We discussed above that a conformational stability of esters is substantially influenced by the interactions between the nonbonded atoms. Obviously, these interactions are affected under protonation when one of the oxygens is replaced by a $O{-}H^+$ bond. If **Ia** is protonated at O_3, the intramolecular $O_2\cdots H_6$ distance of 2.680 Å remains almost unchanged and there takes place a delocalization from the $LP(O_2)$ to the $\sigma^*(C_5H_6)$ or $\sigma^*(C_5H_7)$ orbitals by about 2 kcal·mol^{-1}. Protonations of **IIa** and **IIIa** at O_2 yield rotations of the CH_2F and CHF_2 groups, transforming the $C_5{-}F$ bonds to a nearly *gauche* position (Figure 4). This rotation favors an $O_2H^+\cdots F$ intramolecular interaction provided by short $H^+\cdots F$ distances ∈ 2.137−2.873 Å and the non-negligible delocalization of the LPs of the F atom(s) to the $\sigma^*(O_2H^+)$ orbital equal to 4.5 kcal·mol^{-1} in **IIa**(O_2H^+) and 1.8 kcal·mol^{-1} in **IIIa**(O_2H^+). The fact that this intramolecular interaction definitely exists is confirmed by a significant $\sigma^*(O_2H^+)$ occupation in these systems ranging from 0.010 e in the two **Ia**-protonated systems to 0.020 e in **IIa**(O_2H^+) and 0.015 e in **IIIa**(O_2H^+) (Table 6). Let us also mention that, in protonated methoxycarbonyl systems, the formation of the intramolecular hydrogen bond leads to significant enhancement of basicity.[42]

The charge transfer from the proton to the ester varies between 0.45 and 0.47 e. It is slightly larger, by 0.01−0.02 e, for protonation at O_2. Apparently, it is independent of the substituents implanted on C_5. Protonation at O_2 results in a larger decrease of the charge on O_3 than on O_2, and the reverse holds when O_3 is protonated. In both cases, the charges on the H and F atoms bonded to the C_1 and C_5 carbons decrease. Notice an absence of correlation between the PAs and the charges on the excess proton, similar to that of protonated fluorethers[43] or the negative charges on the C=O groups, similar to that of protonated aliphatic aldehydes and ketones.[44]

Let's now turn to the geometrical and NBO analysis of the protonation at O_2 and O_3 in the $O_2{=}C_1H_4O_3$ part of the

Table 6. Selected NBO Features of the Most Stable Ia, IIa, and IIIa Conformers of Methyl Formate Derivatives Protonated at the O_2 and O_3 Atoms[a]

	Ia(O_2H^+)	Ia(O_3H^+)	IIa(O_2H^+)	IIa(O_3H^+)	IIIa(O_2H^+)	IIIa(O_3H^+)
Charge[b]						
C_1	0.783	0.707	0.729	0.715	0.793	0.719
	-0.101	*-0.025*	*-0.089*	*-0.025*	*-0.105*	*-0.031*
O_2	−0.559	−0.371	−0.549	−0.345	−0.537	−0.340
	-0.068	*-0.220*	*-0.016*	*-0.220*	*-0.022*	*-0.219*
H_4	0.218	0.198	0.218	0.210	0.223	0.216
	-0.107	*-0.087*	*--0.109*	*-0.091*	*-0.098*	*-0.091*
O_3	−0.413	−0.582	−0.453	−0.619	−0.472	−0.650
	-0.135	*-0.034*	*-0.103*	*-0.065*	*-0.097*	*-0.081*
C_5	−0.230	−0.187	0.411	0.406	0.856	0.922
	0.020	−0.023	−0.013	−0.018	0.015	−0.041
H_6	0.214	0.227	0.206	0.195	-	-
	-0.028	*-0.043*	*-0.058*	*-0.049*	*-0.049*	*-0.038*
H_7	0.214	0.220	-	-	-	
	-0.028	*-0.034*	-	-	-	-
H_8	0.246	0.235	0.218	0.210	0.190	0.179
	-0.062	*-0.049*	*-0.057*	*-0.049*	*-0.049*	*-0.038*
F_7			−0.346	−0.310	−0.327	−0.302
			-0.032	*-0.068*	*-0.030*	*-0.055*
H^+	0.530	0.554	0.542	0.552	0.540	0.554
Hybridization						
(1)$C_1(O_2)$	31.7	28.3	23.0	35.4	20.6	28.3
	-4.6	*-6.0*	*-12.4*	*0*	*-11.7*	*-4.0*
(2)$C_1(O_2)$	-	9.0	8.5	1.8	7.5	5.3
		9	*7.7*	*1*	*3.5*	*1.3*
(1)$C_1(O_3)$	32.1	21.0	31.6	23.5	31.6	23.3
	2.5	*8.6*	*8.0*	*7.5*	*3.0*	*-5.3*
(2)$C_1(O_3)$	pure *p*	-	-	-	-	-
$C_1(H_4)$	36.5	41.8	36.4	40.1	36.6	40.1
	1.8	*7.1*	*1.0*	*4.7*	*0.9*	*4.4*
$C_5(O_3)$	18.1	16.6	19.5	17.9	20.3	18.6
	2.8	*4.3*	*3.2*	*4.8*	*3.9*	*5.6*
Hyperconjugation energy						
LP(2)$O_2 \rightarrow \sigma^*(C_1O_3)$	9.2	71.0	10.2	89.7	10.4	98.7
	-23.5	*38.3*	*-25.0*	*54.5*	*-25.9*	*62.4*
$\rightarrow \pi^*(C_1O_3)$	*80.9*	-	-	-	-	-
LP(2)$O_2 \rightarrow \sigma^*(C_1O_2)$						*15.1*
LP(1)$O_3 \rightarrow \sigma^*(C_1O_2)$[d]	11.2	1.1	18.9	11.4	20.7	7.9
	4.5	*1.1*	*12.4*	*4.9*	*14.6*	*7.9*
LP(1)$O_3 \rightarrow \pi^*(C_1O_2)$[d]	0	7.6	42.6	0	35.4	0
	-50.4	*-42.8*	*-2*	*-40.6*	*4.1*	−31.3
$\pi^*(C_1O_2) \rightarrow \sigma^*(C_1O_2)$			*73.2*		*91.1*	
$\sigma^*(C_1O_3) \rightarrow \sigma^*(C_5O_3)$		8.9		5.6		8.3
LP(3)F_6[b] $\rightarrow \sigma^*(O_3C_5)$			16.0	20.1	15.0	19.9
			3.5	*13.6*	*8.5*	*12.8*
LP(3)$F_7 \rightarrow \sigma^*(C_5O_3)$					15.5	19.3
					9.2	*12.2*
Occupation of antibonding orbitals						
$\sigma^*(C_1O_2)$[c]	0.031	0.045	0.130	0.020	0.136	0.021
	+0.017	*0.032*	*0.114*	*0.004*	*0.106*	*-0.007*
$\pi^*(C_1O_2)$	0	0.016	0.240	0.050	0.210	0.054
	-0.196	*-0.180*	*0.0081*	*-0.109*	*0.067*	*-0.089*

dx.doi.org/10.1021/jp202981m |*J. Phys. Chem. A* 2011, 115, 12586–12601

Table 6. Continued

	Ia(O_2H^+)	Ia(O_3H^+)	IIa(O_2H^+)	IIa(O_3H^+)	IIIa(O_2H^+)	IIIa(O_3H^+)
$\sigma^*(C_1O_3)$	0.032	0.243	0.039	0.290	0.038	0.301
	-0.064	*0.147*	*-0.069*	*0.182*	*-0.070*	*0.193*
$\pi^*(C_1O_3)$	0.294	0	0	0	0	0
$\sigma^*(C_1H_4)$	0.026	0.047	0.025	0.044	0.025	0.043
	-0.037	*-0.016*	*-0.036*	*-0.017*	*-0.035*	*-0.017*
$\sigma^*(C_5O_3)$	0.019	0.018	0.065	0.082	0.120	0.140
	-0.001	*-0.002*	*+0.012*	*+0.031*	*+0.043*	*+0.063*
$\sigma^*(O_2H^+)$	0.010	0.010	0.020	0.011	0.015	0.011

[a] Charge (e), hybridization (% s-character), hyperconjugation energies (kcal·mol^{-1}), σ^* occupation (e). Variations induced by protonation (in italics). [b] Negative sign indicates a decrease of the NBO charge. [c] C_1 atom with the highest s-character. [d] In **IIa**(O_2H^+) and **IIIa**(O_2H^+) protonated systems, two O_3 LPs are involved in the delocalization and the values represent the sum of the two contributions.

molecules. Above, it is discussed that the C_1-H_4 bond length is mainly governed by the $\sigma^*(C_1H_4)$ occupation. On the other hand, protonation, no matter where it occurs, either at O_2 or at O_3, causes a marked contraction of the C_1-H_4 bond, though in the O_3-protonated species an increase, by 4−7%, of the s-character of the $C_1(H_4)$ atom is observed. In the isolated and protonated systems, the C_1-H_4 distances vary within a broad range, between 1.1041 and 1.0867 Å, and obey the following relation:

$$r(C_1H_4) = 4.95X^2 - 0.144X + 1.0879 \quad (R = 0.997) \quad (n = 12) \tag{2}$$

where X = $\sigma^*(C_1H_4) - 1.5 \times 10^{-2}$ [s-character $C_1(H_4)$], R is the correlation coefficient, and n is the number of points. This correlation is illustrated in Figure 6. Interestingly, for some complexes of the formate ion and proton donors, the blue shift of the ν(CH) vibration depends on the σ^*(CH) occupation,[45] though the C−H bond is not directly involved in the hydrogen bonding interaction, thus, validating the model of the intramolecular negative response.[17h,18a] It is worth noticing that, when the C−H bond is involved in a hydrogen bonding interaction, the hybridization seems to be more important in determining the C−H distance than the σ^*(CH) occupation. Further, the coefficients of the dual expression eq 2 have been shown to depend also on the nature of the proton donor and the proton acceptor.[32]

The comparison of the $C_1{=}O_2$ and C_1-O_3 bonds reveals a couple of remarkable features. Indeed, in **Ia**, the $C_1{=}O_2$ distance is shorter than the C_1-O_3 one by 0.143 Å. In **Ia**(O2H$^+$), the $C_1{=}O_2$ bond is 0.021 Å longer than the C_1-O_3 one. The NBO analysis we conduct shows that the $\pi^*(C_1{=}O_2)$ occupation becomes negligible in **Ia**(O2H$^+$) and is replaced by the $\pi^*(C_1O_3)$ one of 0.294 e. In this cation, we observe a rather strong LP(2)$O_2 \rightarrow \pi^*(C_1O_3)$ hyperconjugation energy amounting to 81 kcal·mol^{-1}.

Hence, the bonding patterns of three O_2, C_1, and O_3 atoms are represented as $O_2-C_1{=}O_3$, which is in agreement with the occupancy of the $C_1{=}O_2$ and C_1O_3 bonds.[46] In **IIa**(O_2H^+) and **IIIa**(O_2H^+), the bonding trends are distinguishably different: the $C_1{=}O_2$ and C_1-O_3 bond lengths are nearly equal in **IIa** and the $C_1{=}O_2$ bond is slightly shorter than the C_1-O_3 bond in **IIIa**. Their protonations lead to a strong decrease of the LP(2)$O_2 \rightarrow \sigma^*(C_1O_3)$ delocalization by ∼25 kcal·mol^{-1} and its replacement by a strong $\pi^*(C_1O2) \rightarrow \sigma^*(C_1O2)$ delocalization equal to 73.2 kcal·mol^{-1} in **IIa** and 91.1 kcal·mol^{-1} in **IIIa**.

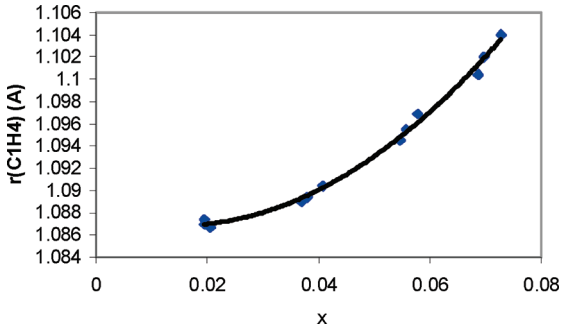

Figure 6. $r(C_1H_4)$ as function of X = $\sigma^*(C_1H_4) - 1.5 \times 10^{-2}$ [s-character $C_1(H_4)$] via eq 2. It definitely shows that the C_1-H_4 bond lengths of the studied systems are largely determined by the $\sigma^*(C_1H_4)$ occupation, though a small effect of the hybridization must be taken into account as well.

In the O_3-protonated systems, the most important effect of the interaction with a proton is a significant growth of the LP(2)$O_2 \rightarrow \sigma^*(C_1O_3)$ hyperconjugation energy, from 38 to 62 kcal·mol^{-1}. It is markedly larger in the fluorinated systems. As discussed in this subsection, the $C_1{=}O_2$ and C_1-O_3 distances vary within a broad range in the protonated systems. A comparison with the neutral molecules allows us to predict these two distances as a function of the NBO characteristics, more specifically as a function of the hyperconjugation energies (HYPE). The $C_1{=}O_2$ bond length correlates with the Σ_{HYPE} by means of the equation

$$r(C_1{=}O_2) = 1.146 + 0.9 \times 10^{-3}\Sigma_{HYPE} \quad (R = 0.984) \quad (n = 14) \tag{3}$$

where Σ_{HYPE} is defined as the sum of the hyperconjugation energies from the LPs of O_2 and O_3 to the $\sigma^*(C_1{=}O_2)$ or $\pi^*(C_1{=}O_2)$ orbitals that also includes the very large $\pi^*(C_1O_2) \rightarrow \sigma^*(C_1O_2)$ delocalization in the protonated complexes **IIa** and **IIIa**. Interestingly, the value of the intercept is rather close to the C=O bond length calculated in CO_2, where no anomeric effect is observed.[47]

A similar correlation is obtained for the C_1-O_3 bond length:

$$r(C_1O_3) = 1.213 + 4.2 \times 10^{-3}\Sigma_{HYPE} \quad (R = 0.998) \quad (n = 14) \tag{4}$$

where Σ_{HYPE} is the sum of the delocalization energies from the LP(2)O_2 to the $\sigma^*(C_1O_3)$ orbitals. Equations 3 and 4 are illustrated in Figures 7 and 8.

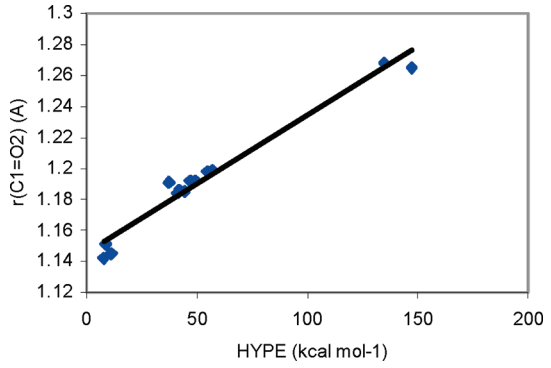

Figure 7. $r(C_1{=}O_2)$ as a function of Σ_{HYPE}.

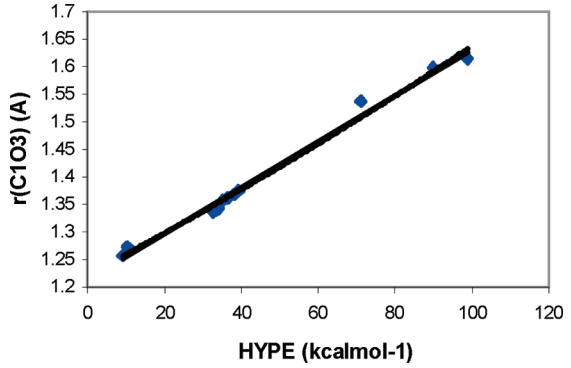

Figure 8. $r(C_1O_3)$ (Å) as a function of Σ_{HYPE} (kcal·mol^{-1}).

Protonation naturally elongates the $O_3{-}C_5$ bonds, particularly in **IIa**(O_3H^+) and **IIIa**(O_3H^+). This effect originates from increase of the $\sigma^*(O_3C_5)$ occupation by 0.012 - 0.063 e which in turn results from the large increase of the LP(3)(F_6) or LP(3)$F_7 \rightarrow \sigma^*(O_3C_5)$ delocalization. This again illustrates the high π-donor ability of the F atom(s) in these systems. Finally, note a strong decrease, by ca. 10 kcal·mol^{-1} of the delocalization of the LP(1)O_2 to the RY* orbital of the C_1 atom under protonation at O_2.

3C. Interaction of Methyl Formate Derivatives with HF. The present subsection focuses on the interaction between the ester derivatives and the HF molecule. We discuss: first, the conformational changes caused by this interaction and second, the hydrogen bond energy as a function of the proton acceptor ability of the esters. Figure 9 gathers all minimum-energy structures of the complexes formed between the different conformers of methyl formate and its mono and difluoro derivatives and HF. The following three scenarios of this interaction are observed: Scenario 1, Interaction with O of the C═O group; Scenario 2, Interaction with O of the CH_3O group; Scenario 3, HF acts as a proton donor to F of the fluorinated esters.

Scenarios 1 and 2 result in the formation of the F−H···O hydrogen bond, whereas scenario 3 results in the F···H−F one. Within scenarios 1 and 2, no marked changes on the conformational manifolds of the esters and of **IIIa** and **IIIb** complexes are detected. While interacting with HF, **IIIc** undergoes a small distortion of the staggered structure where $\angle C_1O_3C_5H_8$ increases to 13° and the **IIa** and **IIb** rotamers arrive at the same distorted structure with $\angle O_1C_3C_5H_6 = 155.7°$; namely, the rotamer **IIa**, slightly more stable by ∼1.3 kcal·mol^{-1}, converts directly to this structure, whereas **IIb** throughout the transition structure.

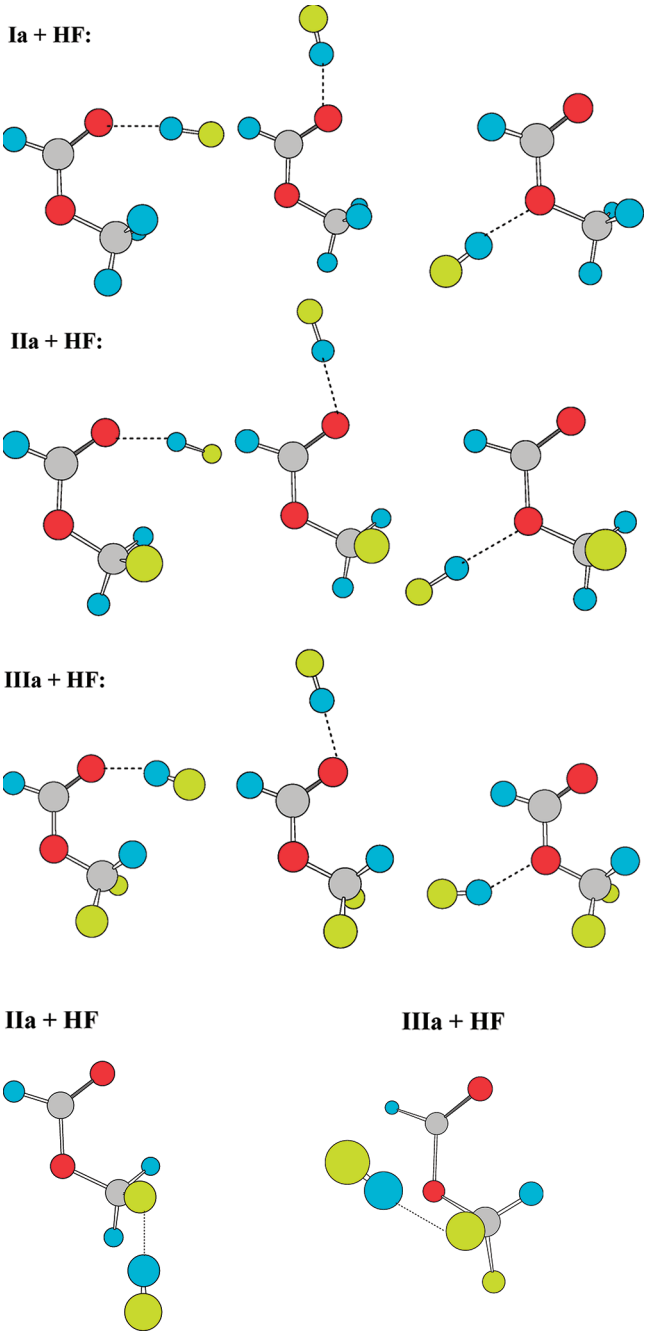

Figure 9. Most stable complexes formed by the **Ia**, **IIa**, and **IIIa** conformers and the HF molecule. The geometrical characteristics of these complexes are given in Table S2 of the Supporting Information.

Table 7 gathers the key information on scenarios 1−3, including the hydrogen bond energies, the intermolecular distances, the geometric changes in the H−F, $C_1{-}H_4$, and C═O bonds, and the frequency shifts of the corresponding stretching vibrations. All geometric data for the most stable conformers **Ia**, **IIa**, and **IIIa** complexed with HF via scenarios 1 and 2 are presented in Table S2. The binding energies of the F···HF complexes that appear in scenario 3 fall in the interval of ∼3−4.4 kcal·mol^{-1}.

Because, according to eq 1, the PA(O_2) > PA(O_3), the O_2···HF complexes are stronger the O_3···HF ones. Similar conclusions

Table 7. Interaction of Methyl Formate and its Mono and Difluorinated Derivatives with HF: Hydrogen Bond Energies (kcal·mol^{-1}), Intermolecular Distances, Variation of the HF, C_1-H_4 and C=O Distances (Å), and Frequency Shift of the ν(HF), $\nu(C_1H_4)$, and ν(C=O) Vibrations (cm^{-1})[a]

	Complexes Formed on the O_2 and O_3 Atoms					
O=CHOCH$_3$	Ia^c	Ia^t	Ia^m	Ib^c	Ib^t	Ib^m
$-E_{HB}$	9.32	9.05	5.94	9.58	9.11	6.05
r(O···H)	1.677	1.691	1.739	1.675	1.716	1.805
Δr(HF)[b]	0.0221	0.0202	0.0145	0.0231	0.0190	0.0121
$\Delta\nu$(HF)[b]	−490	−444	−335	−511	−422	−278
$\Delta r(C_1H_4)$	−0.0028	−0.0025	−0.0011	−0.0040	−0.0037	−0.0013
$\Delta\nu(C_1H_4)$	38	33	18	48	45	30
$\Delta r(C_1{=}O_2)$	0.010	0.009	−0.006	0.009	0.010	−0.004
$\Delta\nu(C_1{=}O_2)$	−41	−33	22	−48	−45	18
O=CHOCH$_2$F	IIa^c	IIa^t	IIa^m	IIb^c	IIb^t	IIb^m	IIc^c	IIc^t	IIc^m
$-E_{HB}$	7.94	7.52	4.72	8.24	8.08	4.51	8.40	7.73	4.81
Δr(HF)	0.0185	0.0173	0.0117	0.0195	0.0192	0.0092	0.0193	0.0178	0.0095
r(O···H)	1.711	1.718	1.779	1.699	1.698	1.850	1.710	1.749	1.855
$\Delta\nu$(HF)	−414	−381	−265	−437	−422	−210	−430	−383	−214
$\Delta r(C_1H_4)$	−0.0020	- 0.0016	−0.0009	−0.0023	−0.0020	−0.0009	−0.0027	−0.0030	−0.0022
$\Delta\nu(C_1H_4)$	29	22	15	32	27	17	39	39	30
$\Delta r(C_1{=}O_2)$	0.010	0.009	−0.005	0.010	0.009	−0.005	0.011	0.009	−0.003
$\Delta\nu(C_1{=}O_2)$	−42	−33	20	−39	−32	18	−46	−38	8
O=CHOCHF$_2$	IIIa^c	IIIa^t	IIIa^m	IIIb^c	IIIb^t	IIIb^m	IIIc^c	IIIc^t	IIIc^m
$-E_{HB}$	7.04	6.81	3.59	7.42	6.30	3.67	7.35	6.66	3.10
r(O···H)	1.731	1.730	1.893	1.729	1.800	1.802	1.732	1.773	1.977
Δr(HF)	0.0165	0.0166	0.0075	0.0171	0.0106	0.0077	0.0175	0.0133	0.0053
$\Delta\nu$(HF)	−372	−362	−171	−383	−239	−177	−392	−300	−122
$\Delta r(C_1H_4)$	−0.0016	−0.0013	−0.0008	−0.0019	−0.0011	−0.0007	−0.0022	−0.0024	−0.0018
$\Delta\nu(C_1H_4)$	24	18	16	27	21	11	32	30	18
$\Delta r(C_1{=}O_2)$	0.010	0.009	−0.014	0.011	0.008	−0.007	0.021	0.018	−0.010
$\Delta\nu(C_1{=}O_2)$	−42	−34	16	−45	−26	15	−45	−34	8

	Complexes Formed on the F Atoms				
	IIa	IIc	IIIa	IIIb	IIIc
E_{HB}	−4.40	−4.42	−3.05	−2.96	−3.40
Δr(HF)	0.0078	0.0087	0.0048	0.0044	0.0048
$\Delta\nu$(HF)	−170	−184	−100	−92	−99
$\Delta r(C_1H_4)$	−0.0011	−0.0017	−0.0024	−0.0015	−0.0031
$\Delta\nu(C_1H_4)$	13	33	22	20	35

[a] Superscripts c, t, and m refer to the complexes formed at $C_1{=}O_2$ in the *cis* or *trans* position to the C_1-H_4 bond and to the complexes at OCH_3. [b] Isolated HF, r(HF) = 0.9221 Å, ν(HF) = 4091 cm^{-1}.

have been drawn for the interaction formic acid−HF[9] and methylacetate−HF.[7] As expected, the energies of these bonds decrease with a number of F atoms implanted on the esters. Moreover, the binding energies of the O_2···HF and O_3···HF complexes do not reveal any noticeable dependence on the conformation of the esters and vary only within 0.5 kcal·mol^{-1}. The same conclusion can be extracted from a theoretical investigation of the interaction between methyl formate and water, showing that the binding energies are slightly larger, about 0.5 kcal·mol^{-1}, for the *E* conformer than for the *Z* one when the water molecule occupies the *cis* position. The reverse holds if the water molecule is in *trans* position. The binding energies for the O_2···HF and O_3···HF complexes correlate with the PAs of the respective O atoms (kcal·mol^{-1}) by means of the following relation:

$$-E_{HB} = 0.169\ PA - 22.7 \quad (R = 0.961) \quad (n = 25) \tag{5}$$

that is illustrated in Figure 10. For the studied systems, the binding energies appear to be a linear function of the corresponding $\Delta\nu$(HF) shifts (in cm^{-1})

$$E_{HB} = 0.017\Delta\nu(HF) + 1.08 \quad (R = 0.970) \quad (n = 24) \tag{6}$$

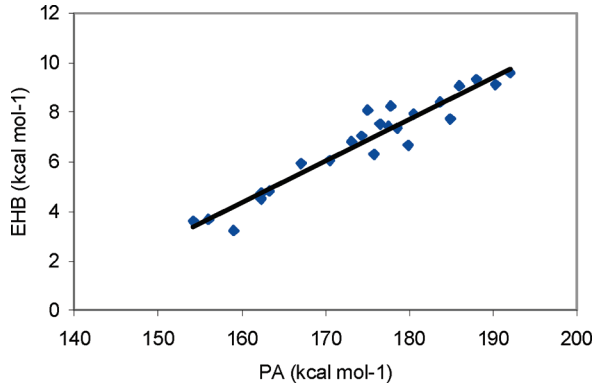

Figure 10. $-E_{HB}$ as function of PA (HF···O H-bond).

In scenario 1, the $C_1{=}O_2$ bond elongates along with a red shift of the $\nu(C_1{=}O_2)$ mode. The reverse trend is predicted for scenario 2. The interaction with HF results in moderate blue shifts of 11−50 cm^{-1} of the $\nu(C_1H_4)$ vibration, the shifts being lower when the proton donor molecule interacts with the O_3 atom. Within a broad class of relevant systems, involving the protonated and hydrogen-bonded molecules investigated in the present work, we establish the following correlation between the contraction of the $C_1{-}H_4$ bonds and the corresponding blue shifts

$$-\Delta r(C_1H_4) = 6 \times 10^{-5}\Delta\nu(C_1H_4) + 0.0002 \quad (r = 0.984) \quad (n = 30) \qquad (7)$$

eq 7 correctly predicts the blue shift of 56 cm^{-1} of the ν(CH) mode in the $H_2C{=}O\cdots HF$ complex where the C−H bond is contracted by 0.0035 Å.[16a]

Let us finally discuss the NBO features of one of the HF complexes, namely, the **Ia**^{c}-HF one. They indicate that the overall charge transfer from **Ia** to HF is equal to 0.041 e, much lower than the charge transfer from **Ia** to the proton (0.47e). Therefore, we may anticipate that the variation of the distances and NBO characteristics are significantly smaller for the interaction with HF than for the protonation (Tables 5 and 7). The intermolecular charge transfer from the two LPs of the O_2 atom to σ^*(HF) amounts to 20.8 kcal·mol^{-1} which readily explains the elongation of 0.022 Å and the red shift of 490 cm^{-1} of the ν(HF) vibration. The interaction with HF results in a decrease of the delocalization LPs(O_2) → $\sigma^*(C_1H_4)$ by 4.5 kcal·mol^{-1} and a decrease of the corresponding $\sigma^*(C_1H_4)$ occupation by 0.008 e. These changes lie in agreement with non-negligible blue shift of 38 cm^{-1} of the $\nu(C_1H_4)$ vibration, which is induced by the interaction with HF. It is worth mentioning that eq 2 predicts the C_1H_4 bond length of 1.0944 Å, which is very close to the ab initio value of 1.0941 Å (see Table 7).

4. SUMMARY AND CONCLUSIONS

In the present work, some important properties of methyl formate and its mono and difluoro derivatives have been computationally investigated. Among them are the conformational manifolds, the basicity of the different sites, and the hydrogen bond propensity. The key conclusions of our work are the following:

(I) For the three investigated ester derivatives, the *Z* conformers, including their corresponding rotamers, are more stable than the *E* ones. The difference in their relative stabilities is not too large: within ∼3−5 kcal mol^{-1}. These stabilities depend not only on hyperconjugative interaction but also on the attraction or repulsion between nonbonded atoms, especially in the fluorinated systems.

(II) The PA of the carbonyl O atom is by 15−20 kcal mol^{-1} larger than the PA of the acyl O atom. F-substitutions yield a moderate decrease of the PA of both O atoms. Protonation on the F atom(s) causes a fission of the C−F bond.

(III) Protonation on both O atoms induces a marked contraction of the C−H bond and large blue shifts of the ν(CH) vibration. Quantitative correlations have been deduced between the C−H, C=O, and C−O distances and the NBO features, such as the occupation of relevant antibonding orbitals and hyperconjugation energies. In fact, the ground-state protonated methyl formate can be regarded as a superposition of **Ia**($O_2H^+_{cis}$), originated from the stable *Z* conformer, and **Ib**($O_2H^+_{cis}$), originated from the metastable *E* one. A quite intriguing question then naturally arises: Whether a deprotonation of the ground-state protonated methyl formate yields, with some probability, the metastable *E* conformer? If yes, this would be a first experimental detection of *E*.

(IV) Stable complexes with the HF molecule are formed on both O atoms of the esters. The corresponding binding energies are linearly correlated with the PA of the corresponding O atoms. Classical effects, such as the red shift of the ν(HF) or ν(C=O) vibrations, have been predicted. Hydrogen-bonded complexes characterized by lower stabilities are formed when HF anchors to the F atom(s). These results are fairly correlated with some experimental facts on the complexation of esters with HCl in low-temperature matrices. In particular, under

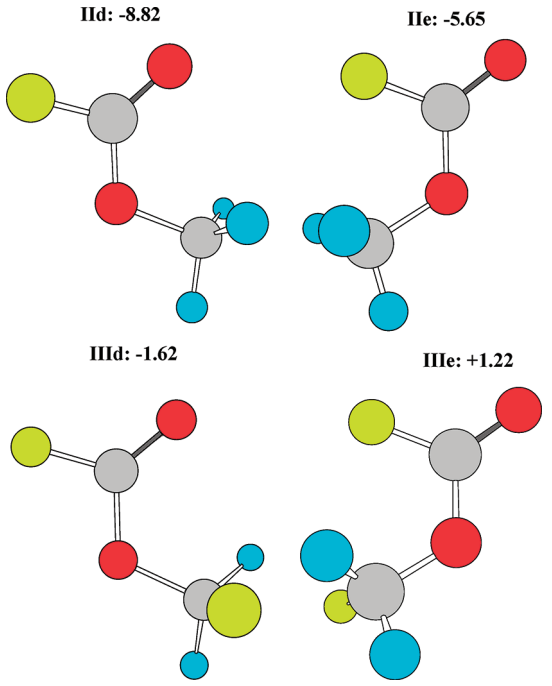

Figure A. The rest of the B3LYP/6-31++G(3df, 3dp) PESs of mono- and difluoro-substitution of methyl formate. The differences in energy (in kcal·mol^{-1}) are taken relative to **IIa** and **IIIa**.

complexation of methyl formate and HCl, red shifts $\Delta\nu$(HCl) = 240 and 360 cm^{-1} of the two ν(HCl) modes relative to ν_o(HCl) of the isolated HCl. were observed.[6a,b] These modes were assigned to the complexes either formed at the methoxy or carbonyl O atoms. The relative shifts $\Delta\nu$(HCl)/ν_o(HCl), equal to 0.08 for the $O_3\cdots$HCl complex and 0.120 for the $O_2\cdots$HF one, are close to $\Delta\nu$(HF)/ν_o(HF) we have obtained for the HF complexes. By analogy, the two ν(C═O) modes, one shifted to higher, whereas the other to the lower wavenumber, were assigned to the $O_3\cdots$HCl and $O_2\cdots$HCl complexes. Blue shifts of 5−15 cm^{-1} of the ν(CH) and ν(CH_3) vibrations were also assigned to the latter complexes. Note that these blue shifts were intuitively explained by the "*trans* lone pair" effect,[48] which is closely related to the anomeric one quantitatively discussed in the present work.

APPENDIX A. GLOBAL ENERGY CONFORMERS ON PESS OF F-SUBSTITUTED METHYL FORMATES

In fact, the global energy conformers, **IId** and **IIId**, on the PESs of mono- and difluoro-substitution of methyl formate are not the F-substituted CH_3 group rather the F-substituted O═C−H_4 and one hydrogen of CH_3. This is demonstrated in Figure A for the first time and definitely implies that the common F-substituted methyl formates belong to the metastable isomers.

ASSOCIATED CONTENT

Supporting Information. A short summary of the NBO data of the C_5−H_6(F_6), C_5−H_7(F_7), and C_5−H_8 bonds in O_2- and O_3-protonated **Ia**, **IIa**, and **IIIa** is presented in Table S1. Selected geometrical features of the complexes of **Ia**-HF, **IIa**-HF, and **IIIa**-HF are given in Table S2. This material is available free of charge via the Internet at http://pubs.acs.org.

AUTHOR INFORMATION

Corresponding Author

*E-mail: therese.zeegers@chem.kuleuven.be; eugene.kryachko@ulg.ac.be.

ACKNOWLEDGMENT

We gratefully thank Prof. George C. Schatz and Prof. Cherif Matta for the kind invitation to participate in the Festschrift dedicated to Prof. Rich Bader. Reviewers are acknowledged for their valuable comments and suggestions. The calculations reported in the present work were performed on the GRID Cluster at the Bogolyubov Institute for Theoretical Physics of the National Academy of Science of Ukraine.

REFERENCES

(1) (a) Pimentel, C. G.; McClellan, A. L. *The Hydrogen Bond*; W. H. Freeman: San Francisco, CA, 1960. (b) Schuster, P., Zundel, G., Sandorfy, C., Eds. *The Hydrogen Bond. Recent Developments in Theory and Experiments*; North-Holland: Amsterdam, 1976. (c) Jeffrey, G. A.; Saenger, W. *Hydrogen Bonding in Biological Structures*; Springer-Verlag: Berlin, 1991. (d) Scheiner, S. *Hydrogen Bonding: A Theoretical Perspective*; Oxford University Press: New York, 1997. (e) Scheiner, S., Ed. *Molecular Interactions: From van der Waals to Strong Bound Complexes*; Wiley: Chichester, 1997 and references therein.

(2) (a) Slee, T.; Bader, R. W. F. *J. Mol. Struct.: THEOCHEM* **1992**, *255*, 173–188. (b) Carroll, M. T.; Bader, R. W. F. *Mol. Phys.* **1988**, *65*, 695–722.

(3) Bader, R. F. W. *Atoms in Molecules: A Quantum Theory*; Oxford University Press: Oxford, 1990.

(4) (a) Matta, C. F. In *Hydrogen Bonding − New Insights*; Grabowski, S., Ed.; Springer: Dordrecht, 2006; Ch. 9. (b) Grabowski, S. J.; Leszczynski, J. In *Hydrogen Bonding − New Insights*; Grabowski, S., Ed. Springer: Dordrecht, 2006; Ch. 14. (c) Chęcińska, L.; Grabowski, S. J. *Chem. Phys.* **2006**, *327*, 202–208. (d) Grabowski, S. J.; Lipkowski, P. *J. Phys. Chem. A* **2011**, *115*, 4765–4773 and references therein.

(5) (a) Mohallem, J. R. *Theor. Chem. Acc.* **2002**, *107*, 372–374. (b) Kryachko, E. S. *Ibid.* **2002**, *107*, 375–377. (c) Delle Site, L. *Ibid.* **2002**, *107*, 378–380. (d) Bader, R. F. W. *Ibid.* **2002**, *107*, 381–382. (e) Cassam-Chenaï, P.; Jayatilaka, D. *Ibid.* **2002**, *107*, 383–384.

(6) (a) Maes, G.; Zeegers-Huyskens, Th. *J. Mol. Struct.* **1983**, *100*, 305–315. (b) Vanderheyden, L.; Maes, G.; Zeegers-Huyskens, Th. *J. Mol. Struct.* **1984**, *114*, 165–172.

(7) Latajka, Z.; Ratajczak, H.; Zeegers-Huyskens, Th. *J. Mol. Struct.* **1988**, *184*, 201–209.

(8) Rablen, P. R.; Lockman, J. W.; Jorgensen, W. L. *J. Phys. Chem. A* **1998**, *102*, 3782–3709.

(9) Parreira, R. L.; Galembeck, S. E.; Hobza, P. *Chem. Phys. Chem.* **2007**, *8*, 87–92.

(10) Wiberg, K. W.; Laidig, K. E. *J. Am. Chem. Soc.* **1987**, *109*, 5935–5943.

(11) Bond, D.; von Ragué Schleyer, P. *J. Org. Chem.* **1990**, *55*, 1003–1013.

(12) Wiberg, K. B.; Hadad, C. M.; Rablen, P. R.; Ciolowski, J. *J. Am. Chem. Soc.* **1992**, *114*, 8644–8654.

(13) (a) Blom, C. E.; Günthard, Hs. H. *Chem. Phys. Lett.* **1981**, *84*, 267. (b) Demaison, J.; Margules, L.; Kleiner, I.; Csaszar, A. G. *J. Mol. Spectrosc.* **2010**, *259*, 70.

(14) Methyl formate is considered as an organic compound in the star-forming region. See for example: (a) Boechat-Roberty, H. M.; Neves, R.; Fantuzzi, J.; Santos, A. C. F.; Pilling, S. *J. Electron Spectrosc. Relat. Phenom.* **2007**, *156−158*, LXVII–LXVII (A25). (b) Laas, J. C.; Garrod, R. T.; Herbst, E. *Astrophys. J.* **2011**, *728*, 71–79.

(15) (a) Hermann, A.; Trautnner, F.; Gholivand, K.; Vonsen, S.; Varetti, E. L.; Della Vedova, C. O.; Willner, H.; Oberhammer, H. *Inorg. Chem.* **2001**, *40*, 3979–3985. (b) Uchimaru, T.; Tsuzuki, S.; Sugie, M.; Sekiya, A. *Chem. Phys. Lett.* **2003**, *373*, 182–190.

(16) (a) Hagen, K.; Naumov, V. *J. Phys. Chem. A* **1998**, *102*, 7060–7064. (b) Erben, M. F.; Della Vedova, C. O.; Boese, R.; Willner, H.; Oberhammer, H. *J. Phys. Chem. A* **2004**, *108*, 699–706. (c) Zeng, X. Q; Ge, M. F.; Du, L.; Sun, Z.; Wang, D-X *J. Mol. Struct.* **2006**, *800*, 62–68. (d) Aarset, K.; Boldermo, H. G.; Hagen, K. *J. Mol. Struct.* **2010**, *978*, 104–107.

(17) See, for example, (a) Gu, T.; Kar, T.; Scheiner, S. *J. Am. Chem. Soc.* **1999**, *121*, 9411–9422. (b) Masunov, A.; Dannenberg, J. J.; Contraras, R. H. *J. Phys. Chem. A* **2001**, *105*, 4737–4740. (c) Kryachko, E. S.; Zeegers-Huyskens, Th. *Ibid.* **2001**, *105*, 7118–7125. (d) Hermansson, K. *Ibid.* **2002**, *106*, 4695–4702. (e) Delanoye, S. N.; Herrebout, W. A.; van der Veken, B. J. *J. Am. Chem. Soc.* **2002**, *124*, 7490–7498. (f) Li, X.; Liu, L.; Schlegel, H. B. *J. Am. Chem. Soc.* **2002**, *124*, 9639–9647. (g) Alabugin, I. V.; Manoharan, M.; Peabody, S.; Weinhold, J. *J. Am. Chem. Soc.* **2003**, *125*, 5973–5987. (h) Karpfen, A.; Kryachko, E. S. *J. Phys. Chem. A* **2009**, *113*, 5217–5223. (i) Joseph, J.; Jemmis, E. D. *J. Am. Chem. Soc.* **2007**, *129*, 4620–4632 and references therein.

(18) See, for example, (a) Karpfen, A.; Kryachko, E. S. *Chem. Phys. Lett.* **2006**, *431*, 428–433. (b) Chandra, A. K.; Parveen, S.; Das, S.; Zeegers-Huyskens, Th. *J. Comput. Chem.* **2008**, *29*, 1490–1496. (c) Chandra, A. K.; Parveen, S.; Zeegers-Huyskens, Th. *J. Phys. Chem. A* **2007**, *111*, 8884–8896.

(19) Frisch, M. J.; Trucks, G. W.; Schlegel, H. B.; Scuseria, G. E.; Robb, M. A.; Cheeseman, J. R.; Montgomery, J. A., Jr.; Vreven, T.; Kudin, K. N.; Burant, J. C.; Millam, J. M.; Iyengar, S. S.; Tomasi, J.; Barone, V.; Mennucci, B.; Cossi, M.; Scalmani, G.; Rega, N.; Petersson,

G. A.; Nakatsuji, H.; Hada, M.; Ehara, M.; Toyota, K.; Fukuda, R.; Hasegawa, J.; Ishida, M.; Nakajima, T.; Honda, Y.; Kitao, O.; Nakai, H.; Klene, M.; Li, X.; Knox, J. E.; Hratchian, H. P.; Cross, J. B.; Adamo, C.; Jaramillo, J.; Gomperts, R.; Stratmann, R. E.; Yazyev, O.; Austin, A. J.; Cammi, R.; Pomelli, C.; Ochterski, J. W.; Ayala, P. Y.; Morokuma, K.; Voth, G. A.; Salvador, P.; Dannenberg, J. J.; Zakrzewski, V. G.; Dapprich, S.; Daniels, A. D.; Strain, M. C.; Farkas, O.; Malick, D. K.; Rabuck, A. D.; Raghavachari, K.; Foresman, J. B.; Ortiz, J. V.; Cui, Q.; Baboul, A. G.; Clifford, S.; Cioslowski, J.; Stefanov, B. B.; Liu, G.; Liashenko, A.; Piskorz, P.; Komaromi, I.; Martin, R. L.; Fox, D. J.; Keith, T.; Al-Laham, M. A.; Peng, C. Y.; Nanayakkara, A.; Challacombe, M.; Gill, P. M. W.; Johnson, B.; Chen, W.; Wong, M. W.; Gonzalez, C.; Pople, J. A. *Gaussian 03*, Revision A.1; Gaussian, Inc.: Pittsburgh, PA, 2003.

(20) Boys, S. F.; Bernardi, F. *Mol. Phys.* **1970**, *19*, 553.

(21) Reed, A. E.; Curtiss, J. A.; Weinhold, F. *Chem. Rev.* **1988**, *88*, 899–926.

(22) Actually, the conformer *E* is unstable. Though, it can be regarded as a metastable or kinetically long-lived species if there exists the barrier $\mathbf{I}_{saddle}$, which separates *E* from *Z* and which is sufficiently high to confer *E* a substantial lifetime.

(23) Shimanouchi, T. *Tables of Molecular Vibrational Frequencies Consolidated*; National Bureau of Standards: Gaithesburg, MD, 1972; Vol. 1.

(24) Rocha, A. R.; Pimentel, A. S.; Bielschowsky, C. E. *J. Phys. Chem. A* **2002**, *106*, 181–183.

(25) The correlation between the vibrational frequency ν(C═O) and the r(C═O) bond length is the following: $\nu(C{=}O) = -4.9 \times 10^3\, r(C{=}O) + 7.74 \times 10^3$, with $R = 0.968$. The experimental ν(C═O) = 1720 cm^{-1} in the HCOOR derivative, so that our calculated frequencies are predicted to within a scale factor of 0.96. The correlation between the stretching frequency $\nu(C_1H_4)$ and the $r(C_1H_4)$ bond length is given by $\nu(C_1H_4) = -13.1 \times 10^3\, r(C_1H_4) + 17.4 \times 10^3$, where $R = 0.999$.

(26) Topson, R. D. In *Progress in Physical Organic Chemistry*; Taft, R. W., Ed.; Wiley Interscience: New York, 1987; Vol. 16, p 125.

(27) For discussions of the properties of ethers, see, for example, (a) Castiglioni, C.; Gussoni, M.; Zerbi, G. *J. Mol. Struct.* **1989**, *198*, 475–488. (b) Gussoni, M.; Castiglioni, C.; Ramos, M. N.; Rui, M.; Zerbi, G. *J. Mol. Struct.* **1990**, *224*, 445–470. (c) Polavarapu, P. L.; Chiolli, A. L.; Vernice, G. *J. Am. Chem. Soc.* **1992**, *114*, 10953–10955. (d) Polavarapu, P. L.; Zhan, C.; Chiolli, A. L.; Vernice, G. G. *J. Phys. Chem. B* **1999**, *103*, 6127–6132. (e) Wiberg, K. B.; Marquez, M.; Castejon, H. *J. Org. Chem.* **1994**, *59*, 6817–6824. (f) Goodman, L.; Pophristic, V. *Chem. Phys. Lett.* **1996**, *259*, 287–295. (g) Pophristic, V.; Goodman, L.; Guchhait, N. *J. Phys. Chem. A* **1997**, *101*, 4290–4297. (h) Radio, S.; Toniolo, P.; Avataneo, M.; De Patto, U.; Marchionni, P.; Castiglioni, C.; Tommasini, M.; Zerbi, G. *J. Mol. Struct.* **2004**, *710*, 151–162. (i) Alabugin, I. V.; Zeidan, T. *J. Am. Chem. Soc.* **2002**, *124*, 3175–3185. (j) Ulic, S. E.; Oberhammer, H. *J. Phys. Chem. A* **2004**, *108*, 1844–1850.

(28) Nam, P. C.; Nguyen, M. T.; Zeegers-Huyskens, Th. *J. Mol. Struct.* **2007**, *821*, 71–81.

(29) See, for example, (a) Kirby, *The Anomeric Effect and Related Stereoelectronic Effects at O*; Springer: New York, 1983. (b) Juaristi, E.; Cuevas, G. *The Anomeric Effect*; CRC Press: Boca Raton, FL, 1995.

(30) Alabugin, I. V. *J. Org. Chem.* **2000**, *65*, 3910–3919.

(31) Roohi, H.; Ebrahimi, A. *J. Mol. Struct.: THEOCHEM* **2005**, *726*, 141–148.

(32) Nguyen, H. M. T.; Nguyen, M. T.; Peeters, J.; Zeegers-Huyskens, Th. *J. Phys. Chem. A* **2004**, *108*, 11101–11108.

(33) Zierkiewicz, W.; Michalska, D.; Zeegers-Huyskens, Th. *Phys. Chem. Chem. Phys.* **2010**, *12*, 13361–13691.

(34) Bent, A. H. *Chem. Rev.* **1961**, *61*, 275–311.

(35) Correlation between the C═O bond length (Å) and the polarity of the C═O bond, Σ_q, is defined as the sum of the absolute values of the charges (e) on the C and O atoms: $r(C{=}O) = -0.21\, \Sigma_q + 0.93$, with $R = 0.968$.

(36) (a) Juaristi, E.; Cuevas, G. *Tetrahedron* **1992**, *48*, 5019–5087. (b) Perrin, C. L.; Armostrong, K. B.; Fabian, M. A. *J. Am. Chem. Soc.* **1994**, *116*, 715–722.

(37) (a) Vila, A.; Mosquera, R. A. *Chem. Phys. Lett.* **2007**, *443*, 22–28. (b) Vila, A.; Mosquera, R. A. *J. Comput. Chem.* **2007**, *28*, 1516–1530.(c) The $MP2_{fc}$ calculated PA = 184.1 kcal·mol^{-1}.

(38) Lias, S. G.; Liebman, J. F.; Levin, R. D. *J. Phys. Chem. Ref. Data* **1984**, *13*, 695.

(39) (a) Martin, R. L.; Shirley, D. A. *J. Am. Chem. Soc.* **1974**, *96*, 5299–5304. (b) Benoit, F. M.; Harrison, D. G. *J. Am. Chem. Soc.* **1977**, *99*, 3980–3984.

(40) (a) Zierkiewicz, W.; Michalska, D.; Zeegers-Huyskens, Th. *J. Mol. Struct.* **2009**, *911*, 58–64. (b) Kryachko, E. S. *Int. J. Quantum Chem.* **2010**, *110*, 104–119. (c) Kryachko, E. S. *Int. J. Quantum Chem.* **2011**, *111*, 1792–1807. (d) Kryachko, E. S. *Int. J. Quantum Chem.* **2011**, in press.

(41) The $\nu(OH^+)$ vibrational frequency is correlated with the corresponding bond length as follows: $\nu(OH^+) = 17.74 \times 10^3 - 14.4 \times 10^3\, r(OH^+)$, with $R = 0.984$.

(42) Bouchoux, G.; Leblanc, D.; Bertrand, W.; McMahon, T. B.; Szulejko, J. E.; Berruyer-Penaud, F.; Mó, O.; Yanez, M. *J. Phys. Chem. A* **2005**, *109*, 11851–11859.

(43) Vila, A.; Mosquera, R. A. *J. Phys. Chem. A* **2000**, *104*, 12006–12013.

(44) Graña, A. M.; Mosquera, R. A. *Chem. Phys.* **1999**, *243*, 17–27.

(45) Zeegers-Huyskens, Th. *J. Mol. Struct.* **2008**, *887*, 2–8 the correlations are obtained using the data in ref 9.

(46) In **Ia**, the occupancy is as follows: (1)C_1(═O_2), 1.999; (2)C_1(═O_2), 1.998; C_1-(O_3), 1.995; LP(1)O_2, 1.985; LP(2)O_2, 1.840. In **Ia**(O_2H^+), the occupancy is equal to C_1(═O_2), 1.998; (1)C_2(O_3), 1.997; (2)C_2(O_3), 1.990; LP(1)O_2, 1.956; and LP(2)O_2, 1.712.

(47) Hartz, N.; Rasul, G.; Olah, G. A. *J. Am. Chem. Soc.* **1993**, *115*, 1277–1283.

(48) Numerous papers discussed the "trans lone pair effect", which can be observed by means of a blue shift of the ν(CH) vibration (so-called Bohlmann bands). See, for example, (a) Bohlmann, F. *Angew. Chem., Int. Ed.* **1957**, *69*, 641–642. (b) Ernstbrunner, E. E.; Hudec, J. *J. Mol. Struct.* **1973**, *17*, 249–256. (c) Barnes, A. J. *J. Mol. Struct.* **1983**, *113*, 259–271. (d) Nelander, B. *Chem. Phys.* **1992**, *159*, 281–289. (e) Castiglioni, C.; Gussoni, M; Zerbi, G. *J. Chem. Phys.* **1985**, *82*, 3534–3539. (f) da Costa, N. B.; Aquino, A. J. A.; Ramos, M. N.; Catiglioni, C.; Zerbi, G. *J. Mol. Struct.: THEOCHEM* **1994**, *305*, 19–33 and references therein.